Issued with PATT Newsletter

spectrum

PPARC

Dwingeloo 1: A New Nearby Spiral Galaxy

MARCH 1995

ISSUE NO. 5

NEWSLETTER OF THE ROYAL OBSERVATORIES

The Royal Observatories

PPARC

Particle Physics and Astronomy Research Council

Royal Greenwich Observatory
Madingley Road
Cambridge CB3 0EZ
England

tel: +44 223 374000
fax: +44 223 374700
internet: **<user>@ast.cam.ac.uk**

Royal Observatory Edinburgh
Blackford Hill
Edinburgh EH9 3HJ
Scotland

tel: +44 31 668 8100
fax: +44 31 662 1668
internet: **<user>@roe.ac.uk**

Isaac Newton Group of Telescopes
Royal Greenwich Observatory
Apartado de Correos 321
38780 Santa Cruz de La Palma
Tenerife
Islas Canarias

tel: +34 22 405500
fax (INT): +34 22 405646
SPAN: **29146::<user>**
internet: **<user>@lpve.ing.iac.es**

Joint Astronomy Centre
660 N. A'Ohoku Place
University Park
Hilo
Hawaii 96720
USA

tel: +1 808 961 3756
answerphone: +1 808 935 4332
fax: +1 808 961 6516
PSS: 315280809053
internet: **<user>@jach.hawaii.edu**

JAC Offices at Hale Pohaku: +1 808 935 9911
JCMT Carousel: +1 808 935 0852
UKIRT Dome: +1 808 961 6091
fax (JCMT): +1 808 935 5493

ING User Manuals: copies may be obtained by contacting Bill Martin at RGO (username **wlm**).

JCMT User Guide: copies may be obtained by contacting Dorothy Skedd at ROE (username **dacs**) or Henry Matthews at JAC (username **hem**).

UKIRT User Manual: copies may be obtained by contacting Dorothy Skedd at ROE (username **dacs**).

UKST User Manuals: copies can be obtained by contacting the UK Schmidt Telescope Unit at ROE (username **ukstu**).

ING on-line documentation (including the LPINFO system) is available via World Wide Web URL **http://www.ast.cam.ac.uk/~lpinfo/**.

JCMT on-line documentation is available from a FILESERV system (**jcmt_info@jach.hawaii.edu**) accessible at the JAC via e-mail and via World Wide Web URL **http:// www.jach.hawaii.edu/JCMT/index.html**.

UKIRT on-line documentation (the UKIRT_INFORM system) is available via World Wide Web URL **http:// www.jach.hawaii.edu/UKIRT/home.html**.

ING service observing: applications should be sent by e-mail to **service@ast.cam.ac.uk** or **service@ing.iac.es**.

JCMT service observing: applications should be sent by e-mail to **jcmtserv@roe.ac.uk**.

UKIRT service observing: applications should be sent by e-mail to **ukirtserv@roe.ac.uk** or **ukirtserv@jach.hawaii.edu**.

UKST photography: applications for new plates (and loans from the Plate Library) should be sent to the UK Schmidt Telescope Unit at ROE. Forms can be obtained from UKSTU and may be submitted at any time.

Spectrum editors: Mark Holmes (username spectrum) and Keith Tritton (username kpt) at RGO and Mark Casali (username mmc) at ROE.

ISSN 1353–7784

contents

features

news

Editorial

Starting with this issue, the biannual PATT newsletter will from now on be produced and distributed together with alternate issues of *Spectrum*. The content of the PATT newsletter remains the same (except for the material previously included as annexes, which has now all been made available through the World-Wide Web or anonymous ftp). However, material specific to PATT, formerly duplicated in both newsletters, will no longer be repeated in *Spectrum*. The PATT secretariat at Swindon retain editorial responsibility for the PATT newsletter.

spectrum is published quarterly in March, June, September and December by the Royal Observatories

Dwingeloo 1: A New Nearby Spiral Galaxy

Fig. 1 – 'True' colour composite image of Dwingeloo 1 (produced by H Ferguson) based on VRI imaging obtained at the Isaac Newton Telescope (with the help of S Hughes and S Maddox, RGO). The frame's size is approximately 6.4 × 8.2 arcminutes. Dwingeloo 1 has a distinct bar with two spiral arms, suggesting an SBb morphology.

The disk of the Milky Way contains gas and dust which obscures about 20% of the extragalactic sky – the so-called "Zone of Avoidance" (ZOA). Nearby galaxies hidden behind the ZOA may have an important influence on the dynamics of the Local Group and its peculiar motion relative to the cosmic microwave background radiation. However, such galaxies suffer extinction by dust and gas at optical wavelengths, and confusion by stars in the infrared. Emission at 21 cm by neutral atomic hydrogen (HI) associated with late-type galaxies may be observed if the velocity of the emission differs from that of the local gas. Thus, it is possible to detect in HI galaxies behind the ZOA which are very difficult to detect at other wavelengths.

The Dwingeloo Obscured Galaxy Survey (DOGS) is a long-term collaboration of British, Dutch and American astronomers to search about 2000 square degrees of the northern Galactic Plane at 21 cm for new galaxies, using the Dwingeloo 25 m radio-telescope (built in 1956, and probably the world's oldest operational radio-telescope). Its members include W Burton (Leiden), H Ferguson (STScI), P Henning (New Mexico), R Kraan-Korteweg (Groningen and Meudon), A Loan, O Lahav and D Lynden-Bell (IoA, Cambridge), and D Moorrees and T Foley (NFRA, Dwingeloo).

The first stage of this project was a 'fast' 5 minute-per-point search of the whole survey area. The first result of this search, in August 1994, was the detection of the radio emission from a new galaxy, Dwingeloo 1. The position of Dwingeloo 1 (galactic coordinates l = 138.5 degrees; b = –0.1 degrees) coincided with a feature 2 arcminute in diameter previously noted by George Hau (IoA) on a red Palomar Sky Survey plate.

A large spiral galaxy, optically obscured by the Milky Way, has been discovered at a distance of only 3 Mpc.

Follow-up service observations of the new galaxy by the UK Infrared Telescope in Hawaii revealed that Dwingeloo 1 has a bar and possibly spiral arms. Further service observations (with the help of Shaun Hughes and Steve Maddox, RGO) with the Isaac Newton Telescope on La Palma at optical wavelengths revealed Dwingeloo 1 in full glory (see figure), despite the fact that less than 1% of the light emitted in the blue-band from Dw1 reaches the earth due to absorption in the Milky Way. Similar observations by the Wise Observatory in Israel, and the William Herschel Telescope on La Palma confirmed our detection.

The observations suggest that Dwingeloo 1 is a barred spiral galaxy (type SBb), rotating at about 130 km/s, hence with a mass approximately one-third that of the Milky Way. Using the Tully-Fisher relation, it lies at a distance of approximately 3 Mpc from our Galaxy. Its angular and radial proximity to three other well known galaxies – Maffei 1 & Maffei 2 (discovered by Paulo Maffei in 1968) and IC342 – suggest that it is a prominent member of this group of galaxies, one of the neighbouring groups to the Local Group. Dwingeloo 1 is probably one of the most massive galaxies within 4 Mpc. For more details on Dwingeloo 1 and its discovery see Kraan-Korteweg *et al* (*Nature*, **372**, 77, 1994).

The discovery of such a large galaxy close to the Local Group so soon after the start of our survey bodes well for future observations. It is probable that there are many galaxies behind the galactic plane, waiting for us to find them. We are currently combining Palomar plate measurements (utilising the PDS at RGO, with the help of John Pilkington) with optical imaging and spectroscopy at the Wise Observatory and the Isaac Newton Telescope, and with Dwingeloo at 21 cm.

A J Loan, O Lahav, IoA, Cambridge,
R C Kraan-Korteweg, Kapteyn Institute, Groningen and DAEC, Meudon

Summer Vacation Course 1995

The RGO/IoA/MRAO Summer Student Vacation Course will be held again in 1995 at the Royal Greenwich Observatory. The provisional dates for the course this year are 27 June to 11 August. If you require further information on the course, please write to Dr Steve Bell, Vacation Course Officer, Royal Greenwich Observatory, Madingley Road, Cambridge CB3 0EZ, e-mail **sab@ast.cam.ac.uk**.

Steve Bell, RGO

Interstellar Titanium in the Galactic Halo

We have obtained observations of Ti II λ3384 absorption towards 15 distant stars in the galactic halo and the Magellanic Clouds. These new data extend existing surveys of the distribution of Ti^+ to larger distances from the galactic plane than sampled previously, allowing the scale height of titanium, h_{Ti+}, to be determined for the first time. We find it to be 1.5 ± 0.2 kpc, a value which although greater than those of other tracers of neutral gas, is not as large as had been suspected. We interpret the extended distribution of Ti^+ as an indication that its severe depletion in interstellar clouds in the disk is reduced at the lower densities prevailing in the halo. The data are consistent with a simple power-law dependence of the Ti abundance on the ambient density, with exponent $k \simeq 1$. If the model is correct, it implies that refractory elements like Ti are fully returned to the gas phase at distances beyond ~1 kpc from the plane of the Galaxy.

Interstellar medium

The determination of the extent, distribution, and kinematics of the interstellar medium away from the Galactic plane is important both for understanding the physical processes which drive the gas to large distances from the disk and for interpreting the absorption produced by more distant galactic haloes in the spectra of background QSOs. This topic has been an active area of research over the last fifteen years, but the overall picture which has emerged is still incomplete. In particular, it is not yet clear how to bring together the information provided by different tracers of the ISM, which can exhibit significant differences in their distributions.

The scale height of titanium in the galactic halo has been determined for the first time.

Ti^+ is an especially useful probe of the interstellar gas for two reasons. Its ionisation potential (13.58 eV) is so close to that of H^0 that concerns about unobserved ion stages are minimised and the Ti abundance in the neutral gas can be deduced directly. Furthermore,the strongest transition of Ti II, at λ3383.768, is normally unsaturated, allowing a reliable measurement of the column density from the line equivalent width. These properties contrast with those of other interstellar species, such as Ca^+ and Na^0. On the other hand the line occurs in the near-ultraviolet, where atmospheric extinction is high and in general the sensitivity of optical instrumentation is low. Therefore, observations of Ti II absorption in the galactic halo have until recently been limited to the brightest stars and relatively little data are available for distances beyond 1 kpc.

Published measurements

In particular, there are hardly any published measurements of Ti II in the spectra of extragalactic sources, allowing the total column density perpendicular to the galactic plane, $N_0(Ti^+)$, to be deduced. Consequently, previous attempts to determine the scale height of Ti^+ have been inconclusive. In 1989, Edgar and Savage reported a lower limit $h_{Ti+} \geq 2$ kpc, while $h_{Ca+} = 1$ kpc. By adding new observations of 25 sightlines to earlier compilations in a comprehensive study of Ti II and Ca II in the halo, Albert and her collaborators in 1993 confirmed the scale height of Ca^+,

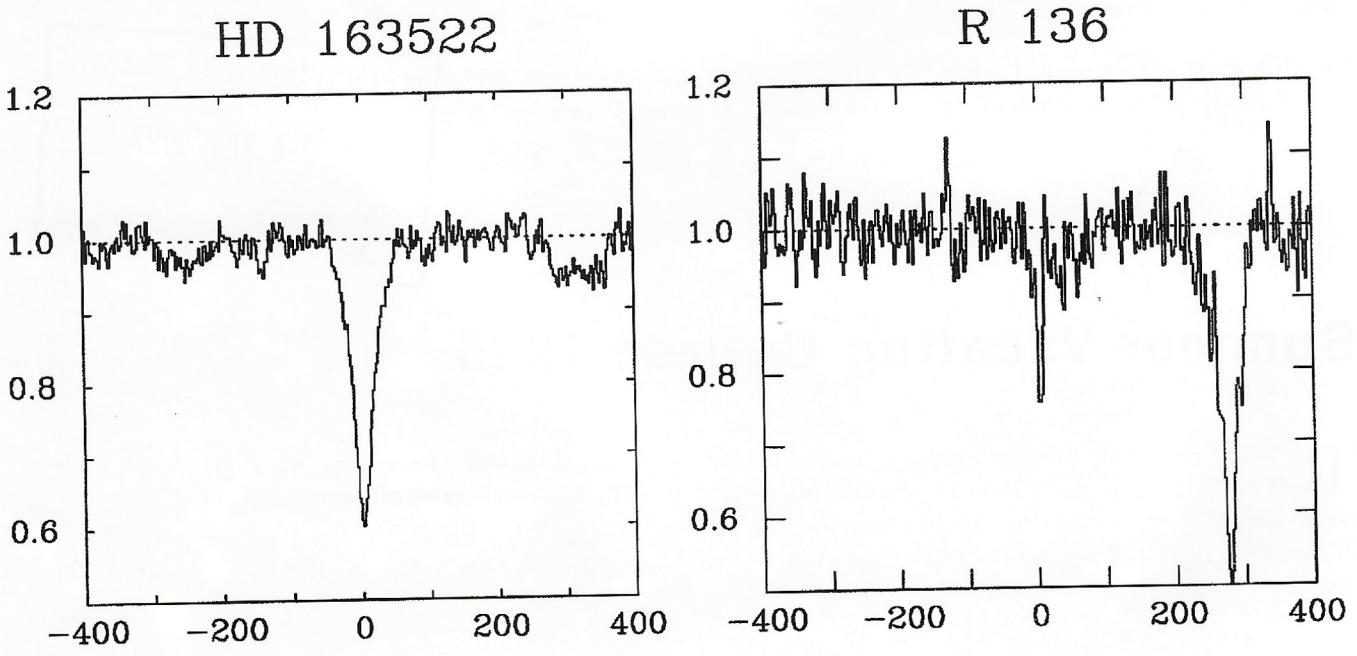

Fig. 1 – Normalised profiles of Ti II λ3383.768 absorption lines towards two of the target stars. The x-axis gives the velocity in km s^{-1} relative to the local standard of rest; the y axis shows the residual intensity on an expanded scale. HD 163522, situated 1.5 kpc distant from the galactic plane, shows a smooth absorption profile. In contrast, R 136, in the Large Magellanic Cloud, exhibits a larger number of components: the absorption in the range 0 to 100 km s^{-1} is due to Milky Way gas; that at 250 to 300 km s^{-1} arises in the LMC itself.

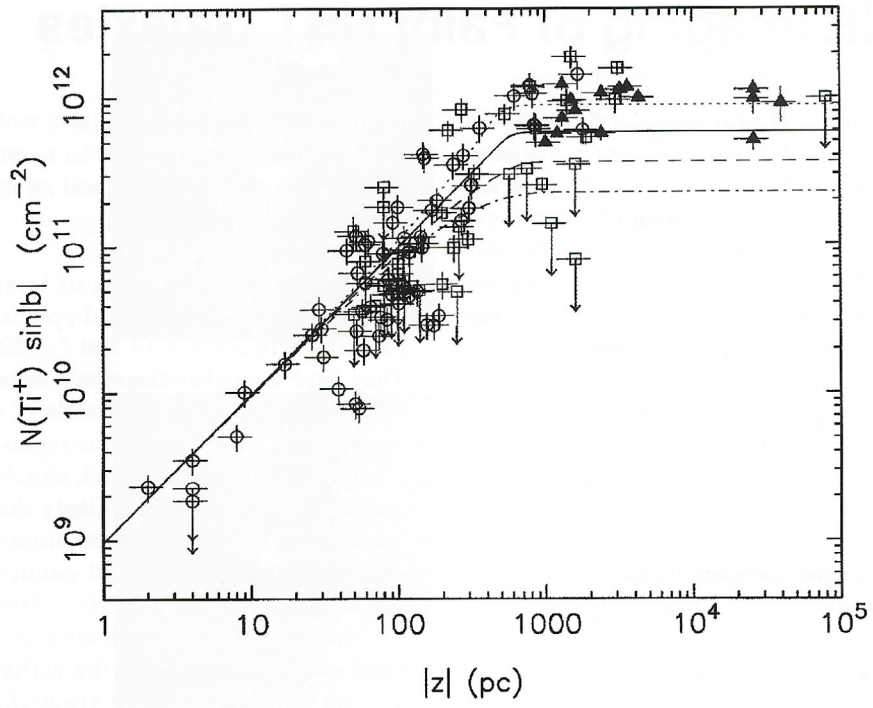

*Fig. 2 – The observed distribution of Ti^+ column densities with distance from the galactic plane is compared with those predicted by our simple model of the density-dependence of the Ti abundance. The y-axis gives the column density normalised to a line of sight perpendicular to the galactic plane; the x-axis gives the distance of the target star from the galactic plane. Circles represent data from Edgar & Savage (1989; ApJ **340**, 762); squares represent data from Albert et al. (1993; ApJS **88**, 81). Triangles indicate our own measurements. The lines plotted on the graph represent different exponents for the relationship of the titanium depletion factor to the local gas density; in descending order, k = –1.2 , –1.0 , –0.8 and –0.6.*

but were still unable to see a turn-over in the vertical distribution of Ti^+.

We have remedied this situation with observations of Ti II absorption in the spectra of 15 stars, all hotter than B4, located beyond 1 kpc from the plane of the Galaxy; four of the stars lie in the Magellanic Clouds. These data extend previous studies of the distribution of Ti^+ in the halo to a largely unexplored region and show that the scale height of Ti^+ is in fact $h_{Ti+} \simeq 1.5$ kpc, greater than that of Ca^+, but not by a large factor.

The data were secured over a period of 5 years, from 1989 to 1994. All but one of the stars were observed with the University College London echelle spectrograph at the coudé focus of the 3.9m Anglo-Australian Telescope at Siding Spring Observatory, Australia. The spectrum of one star, HDE233622, was obtained with the Utrecht echelle spectrograph at the Nasmyth focus of the 4.2m William Herschel Telescope on La Palma, Canary Islands. All the spectra – except those of HD5980 and HD269333 – were recorded with the IPCS, a photon counting detector which, because of its low noise, high quantum efficiency in the ultraviolet and small pixels, is well suited to the present programme. HD5980 and HD269333 were observed in 1994 with a 1024 × 1024 Tektronix CCD. Examples of the spectra are shown in figure 1.

In order to study the distribution of titanium in the Galactic halo we have combined our measurements with those published in the extensive compilations by Edgar and Savage and by Albert and collaborators. The combined sample consists of a total of 116 sight-lines; the new observations presented here increase the number of objects further than 2 kpc from the Galactic plane from 3 to 12. The best-fit exponential distribution of titanium in the halo is found to have a scale height $h_{Ti+} = 1.5$ kpc, and a limiting column density $N(Ti^+) = 1.3 \times 10^{12}$ cm^{-2}.

Contrary to what one might expect, the scale heights of various neutral-phase ions are not equal; in fact, the scale height of Ti^+ is the largest measured so far. This behaviour is generally interpreted to be a consequence of the reduced depletion – and hence enhanced gas-phase abundance – of refractory elements at the low densities which are presumably found away from the disk of the Galaxy. In order to investigate such a relationship, we have collected N(HI) measurements towards the majority of the stars in the sample. We find that the data are consistent with the gas phase abundance of titanium being inversely proportional to the local gas density, as shown in figure 2. In effect, this implies that gas beyond around 1 kpc of the galactic plane should be free of dust depletion. This proposal will be tested in the future by searching for Ti II absorption from individual gas clouds which are known to be far from the plane.

Keith Lipman, IoA, Cambridge
Max Pettini, RGO

Spectroscopy and IR Imaging of Faint HST Galaxies

During this year, an important HST survey project has been under way. The Medium Deep Survey (MDS) is designed to exploit the parallel mode of HST; whenever a primary FOC/FOS observation is made, WFPC-2 is operated simultaneously to snap an image of a random field 4 arcminutes away. Depending on the primary programme the parallel exposures can vary from 2000 seconds for the single orbit, minimum, observation up to many tens of thousands of seconds for the primary exposures which require many orbits.

The MDS team has been particularly interested in the morphological nature of faint galaxies in the field, the survey images being ideal for this purpose, with a view to clarifying the nature of these objects and trying to gain an insight into the 'Faint Blue Galaxy Problem.'

It was well-established in the 1980s that the numbers of faint galaxies increasingly exceed the prediction from a non-evolving galaxy population at faint magnitudes $B > 20$. This was conventionally interpreted as evidence for evolution of galaxies to brighter luminosities at higher redshifts: this might be expected as the systems would be younger and undergoing more vigorous star-formation at these early epochs. Indeed one speculation was they might be protogalaxies at redshifts $\gg 1$.

Technological improvements

The situation has changed radically in the last five years since improvements in spectrograph and CCD technology (*eg* LDSS1 on the AAT, LDSS2 on the WHT, MOSIS on the CFHT) have enabled clear spectra of these faint $B = 22 - 24$ galaxies to be measured (for example the Durham $B = 24$ redshift survey). These show low redshifts for the blue excess population, typically $z \sim 0.5$, indicating luminosities comparable to systems such as the Milky Way. Note however they are much bluer so at longer wavelengths (I and K) they are relatively dimmer.

This population disappears between $z = 0.5$ and $z = 0$, as is evident from the luminosity function work based on these redshift surveys which has been done at Cambridge: the indications are that some combination of density and luminosity evolution of the blue population is required. This fits in with the proposed models: for example the merger model where they disappear through coalescence either into pre-existing larger galaxies or to generate such galaxies themselves. The competing 'exploding-dwarfs' model supposes that the population are dwarf galaxies that were bright at $z = 0.5$ owing to an extreme starburst: this has shut itself off in some way (*eg* supernova winds expel gas from small galaxies) and the population has faded far down the luminosity function (beyond $M_B = -14$ to escape the redshift survey luminosity function constraints at $z = 0$).

Faint galaxies from the Hubble Space Telescope Medium Deep Survey are being used to investigate the faint blue galaxy excess.

From the ground many parameters are available to constrain evolutionary scenarios; redshifts, spectral types and colours in a variety of optical/IR bands have been obtained and confirmed independently by a number of competing groups and models are still degenerate. Now HST has opened up a new dimension in relating this activity to galaxies we can recognise with present-day counterparts: at $z = 0.5$ this sub-kpc morphological structure requires $0.1 - 0.2$ arcsecond resolution which has yet to be achieved from the ground.

This has been the motivation of our MDS survey: the images are sufficiently deep that by 1994 we had assembled a collection of several hundred galaxies selected to $I = 22$ (mean $z = 0.5$) imaged with the MDS. The galaxy counts are complete to $I = 23$: working a magnitude above the completeness limit allows accurate morphological classification. This has been verified by a simulation of placing local galaxies at these high-redshifts and observing them with HST: the results are very similar to our HST images and morphological structure is readily distinguishable.

Our results show the onset of large numbers of faint irregular and peculiar galaxies between $I = 19$ and $I = 22$. They have a number-magnitude slope much steeper than the predictions of a no-evolution model unlike the regular elliptical/spiral systems which closely follow the prediction. It is likely that this increase is the cause of the historic excess in the total ground counts. Interestingly we find a $20 - 30\%$ fraction of multiply-nucleated systems – a result similar to the earlier efforts of Colless *et al* from the ground at 0.6 arcsecond resolution. Obviously they could be galaxy-galaxy mergers caught in the act.

General galaxy population

While we have identified a clear change in the general galaxy population mix we need more information to determine their physical nature: in particular the same spectra and colours mentioned above. And there lies the rub: whilst we have a large sample, the objects, being from random fields, are completely uncorrelated with previous deep redshift surveys. (There are HST programmes to image selected fields from ground-based deep redshift surveys but these will total only a fraction of our objects). To this end we have been using WHT and UKIRT to secure new spectra and optical-IR colours of our new MDS sample. We have had a successful run at each telescope and have more scheduled in May this year. On a typical 4 m run we can get spectra of $10 - 20$ objects a night or observe three of our whole HST fields to $K = 19$. In figure 1 we show examples of our HST images which clearly show the morphological nature of the $I < 22$ galaxies. The accompanying WHT spectra (using the LDSS2 spectrograph as we did for the previous Durham $B = 24$ redshift surveys) show the spectral type associated with each galaxy. The correlation between physical and spectral morphology is generally excellent, ranging from early-type systems with strong HK lines

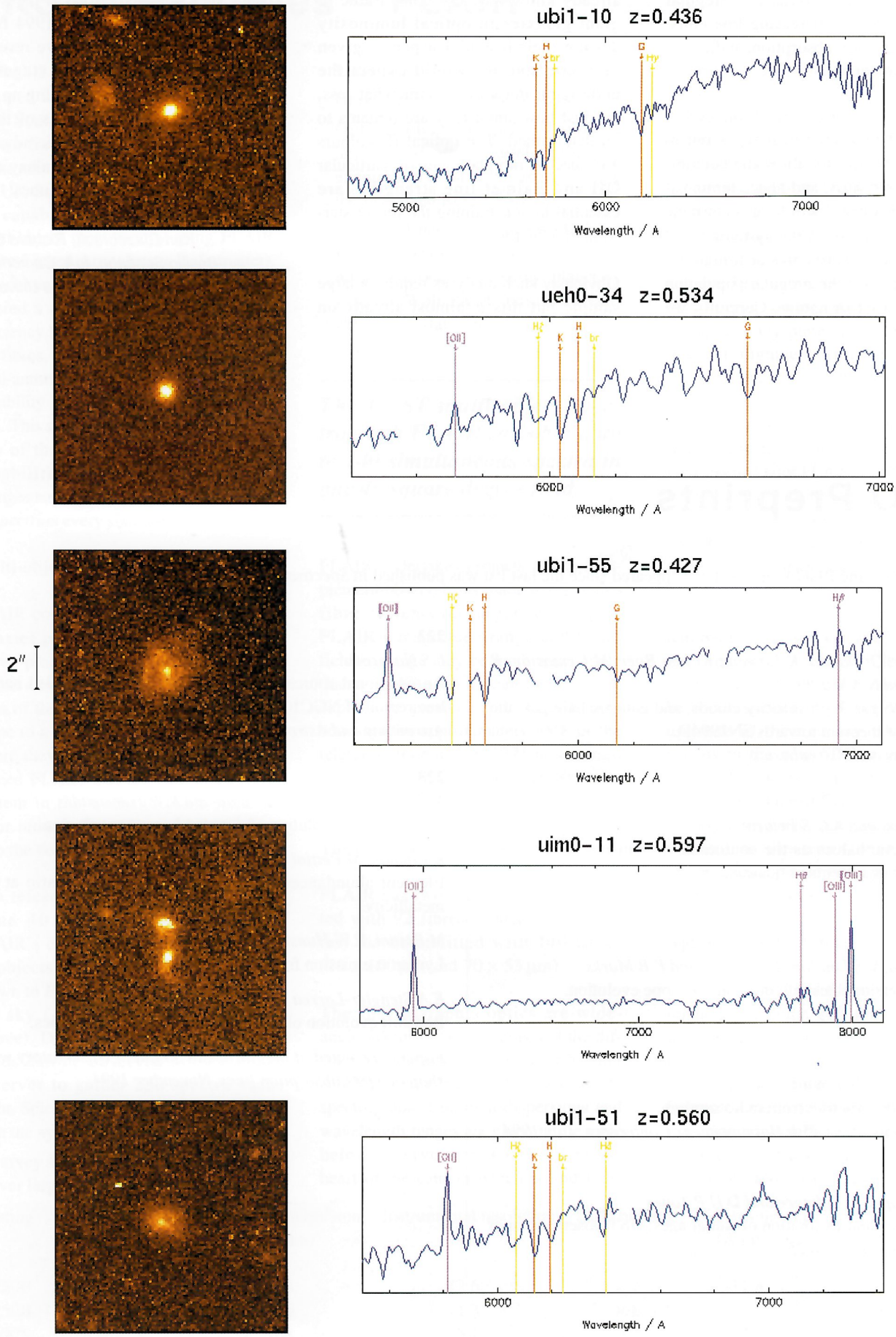

Fig. 1 – Medium Deep Survey HST images of five galaxies from our I < 22 sample (typically I = 21 and z = 0.5). The correlation between physical and spectral morphology is marked: early-type galaxies generally show stronger HK + break lines while as we move down the page to later spiral and irregular types signs of star-formation such as OII emission and Balmer absorption become more evident. Interestingly, object uim 0-11 is clearly tidally interacting and the spectrum shows the strongest emission lines.

and break to later spiral and irregular systems showing increasing line emission and Balmer absorption, indicative of star-formation.

Ultimately we wish to track the evolution of all morphological types out to $z = 0.5$. The spectra allow the determination of redshifts, and hence luminosities. Our K images will let us determine the intrinsic mass of the systems (as K light is least sensitive to star formation) so we can tell if the irregular population is truly dwarf in nature. Certainly we already know they are comparable to giant galaxies in optical luminosity despite their irregular aspect – given they are blue we would expect the underlying mass to be somewhat less, but just how small they are remains to be determined. The optical-IR colours and spectral morphologies (in particular OII and Balmer line strengths) are essential in constraining the recent star-formation history.

Obviously such analyses require a large sample but this is almost already on hand. The combined efforts of the MDS team in the last quarter of 1994 from three successful 4 m runs have resulted in ~90 spectra, in various stages of reduction. More runs are coming up and we fully expect the analyses of these samples to produce a dramatic advance in our understanding of the galaxy content of the universe at earlier times.

Karl Glazebrook, Richard Ellis,
Basilio Santiago, IoA, Cambridge,
Richard Griffiths, Johns Hopkins University

RGO Preprints

The following RGO Preprints have appeared since the last list was published in *Spectrum* No 4.

217
D L King, G Vladilo, K Lipman, K S de Boer, M Centurión, P Moritz and N A Walton
NGC 4526 gas, high velocity clouds, and galactic halo gas: the interstellar medium towards SN1994D.
Astronomy and Astrophysics

218
S M Viegas and A C S Friaça
Hot galactic haloes as the source of the ionising radiation of Lyman limit systems of quasars.
MNRAS

219
M J Sarna, V S Dhillon, T R Marsh and P B Marks
An observational test of common-envelope evolution.
MNRAS

220
C R Benn and J V Wall
Large-scale structure from radio surveys.
Proceedings of the 35th Herstmonceux Conference, July 1994

221
T von Hippel, G Gilmore and D H P Jones
An independent calibration of stellar ages: HST observations of White Dwarfs at $V = 25$.
MNRAS

222
L S Nazarova
An additional source of gas ionisation in the extended narrow line region of NGC1068.
Astronomy and Astrophysics

223
M Pettini, D L King, L J Smith and R W Hunstead
The chemical evolution of damped Lyman α galaxies.

K Lipman, M Pettini and R W Hunstead
Element abundances at high redshifts: the N/O ratio at low metallicity.

M Pettini, R W Hunstead, D L King and L J Smith
Lyman α emission from high redshift galaxies.

E A Stengler-Larrea
Redshift evolution of the carbon abundance in galaxies.

Papers presented at the European Southern Observatory workshop on QSO absorption lines, November 1994

UKSTU Facilities – FLAIR

The 1.2 m UK Schmidt Telescope situated at Siding Spring Observatory, New South Wales, Australia is mainly known for its superb, deep photographs of the southern sky. However since 1985 the UK Schmidt Telescope has also had the capability to carry out wide-field multi-object spectroscopy using FLAIR (Fibre-Linked Array-Image Reformatter). The commissioning of FLAIR II in 1992 offered a sixfold increase in observing efficiency by having three times the original fibres, a purpose-built spectrograph, semi-automatic fibre positioning and the capability of consecutive nightly operation. This article gives an overall description of the current instrument and its capabilities. Updates on hardware changes and applications will be provided in *Spectrum* every six months.

Multi-object spectroscopy

FLAIR collects the light from stars and galaxies by means of some 90 optical fibres placed at the telescope's focus within a modified plate holder. The free ends of the fibres reach out of the telescope to a laboratory bench in the dome where they connect into a spectrograph. Indeed FLAIR was the first multi-fibre system in the world to use a remote, floor mounted spectrograph, and thus reap the benefits of mechanical stability.

The telescope's large field of view, some 40 square degrees, ensures FLAIR's efficiency at obtaining spectra of objects of intermediate magnitude (down to $B = 18$) sparsely distributed on the sky (1 – 10 objects per square degree). During long winter nights two fields can be observed allowing the observer to gather 230 spectra each night. Scientific programmes carried out with the system include

Survey spectroscopy of bright quasars over large areas

Large scale galaxy redshift surveys

Observations of nearby clusters

Optical identifications of objects detected at other wavelengths, for example, the surveys carried out by the IRAS and ROSAT satellites

Studies of particular classes of object in the Magellanic clouds and the nucleus of our own Galaxy: planetary nebulae, Wolf-Rayet stars, Mira variables, flare stars, etc.

The UKST multi-object spectrograph FLAIR can obtain up to 140 simultaneous spectra in one 40 square degree field.

FLAIR undertakes projects which complement observations made using multi-fibre systems on larger telescopes. FLAIR's magnitude range and wide-field coverage may be more appropriate than a system with a small field of view capable of greater depth. FLAIR now accounts for approximately 35% of the telescope time and in 1994 it was used to make observations of over 6000 target objects.

The hardware

FLAIR has two plate holders, one fitted with 92 fibres (100 μm in diameter) the other fitted with 140 fibres (70 × 100 μm and 70 × 55 μm).

The spectrograph's optics are wide-angle Schmidt-type systems and the diffraction gratings are shared with other AAO instruments such as the RGO spectrograph. Common dispersions and wavelength ranges are given in the table below. A cryogenic CCD sits at the heart of the camera which is under the control of a PC situated in the Schmidt common room.

A plate scale of 67 arcseconds/mm and fibre diameters of 55 or 100 μm (3.7 and 6.7 arcseconds) means that the fibres need to be positioned with an accuracy of better than 10 μm to intercept fully the light from each target object. This is achieved by cementing the fibres via micro-prisms on to a standard size photographic copy plate of the target field in exact alignment with the images of the selected objects visible on the plate.

The positioning is carried out using a semi-automatic fibre-positioner 'auto-Fred' named after FLAIR's instigator and first project scientist Fred Watson. "Fibring up" takes about 4 – 6 hours for 100 fibres and is usually carried out during daytime prior to each night's observing.

Future enhancements to the FLAIR system include a new CCD (EEV 02 – 06) with increased sensitivity in the blue (about a gain of one magnitude), due to be commissioned in early 1995, and an upgrade of the existing BK7 micro-prisms to the new SP5 variety which offer a 30% increase in efficiency. The current and planned CCD both have 578 × 400 22 μm pixels and readout noise of 10 and 8 electrons respectively. Observations should be kept within the range 3800 – 9500Å.

Applying for FLAIR time

FLAIR is scheduled for runs of up to 7 nights per lunation with the time in any one semester being divided equally between applications submitted to the two (UK and Australian) halves of the Schmidt Telescope Panel. Programmes requiring any number of nights may be submitted and a run might be shared between two or more projects.

Grating	Blaze direction	Reciprocal dispersion (Å/mm)	Instrumental resolution (Å)	CCD binning	CCD resolution (Å/pixel)	Spectral range (Å)
250B	camera	268	12.6	×2	11.8	3400
250B	collim	286	11.3	×1	6.3	3620
600V	camera	108	5.1	×2	4.7	1360
600V	collim	122	4.5	×1	2.7	1540
1200B	camera	49	2.6	×2	2.2	620
1200B	collim	62	2.1	×1	1.4	790

Table 1 – Details of some of the available gratings

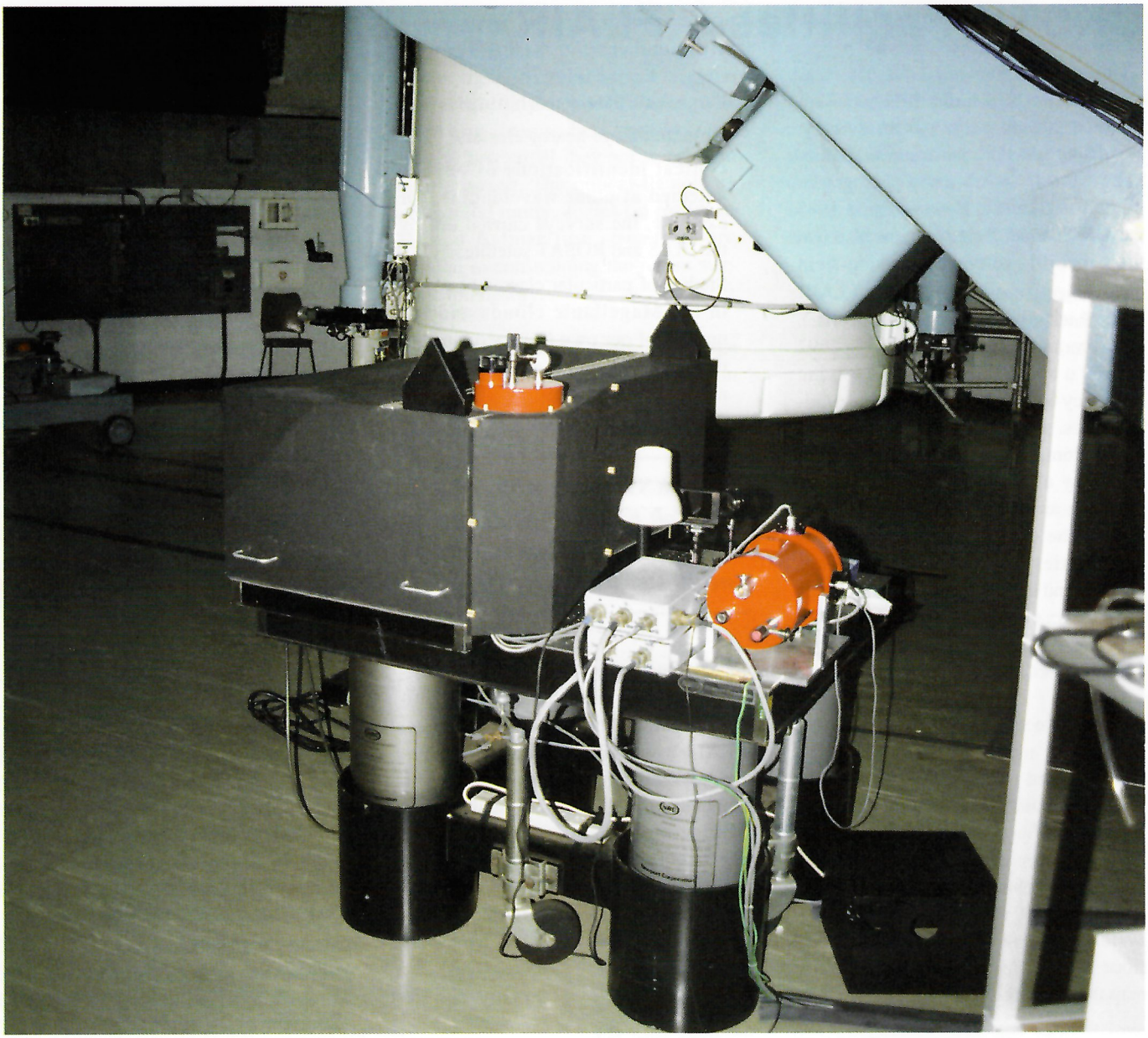

Fred Watson

Fig. 1 – The UK Schmidt Telescope with FLAIR.

How to apply

Currently applications are sought twice a year for the two semesters running from February – July (Semester A) and August – January (Semester B). The deadlines match those used by the Australian Time Assignment Committee (ATAC) and are announced in the AAO newsletter.

Applicants are encouraged to seek advice and raise queries before submitting proposals. Requests for further information and FLAIR forms, and completed applications should be sent to either

UK applicants

Mike Read
U.K. Schmidt Telescope Unit,
Royal Observatory,
Blackford Hill,
Edinburgh EH9 3HJ
Tel 031 668 8328
Fax 031 662 1668
e-mail **ukstu@roe.ac.uk**

Australian applicants

Quentin Parker
AAO
Coonabarabran
NSW 2357
Australia
Tel 061 68 42 6316/6291
Fax 061 68 84 2298
e-mail **qap@aaocbn3.aao.gov.au**

Other nationalities can apply to either panel. The Latex application form, a template file and a Fortran program to combine the two are also available via anonymous ftp to 192.108.120.17. The three files are in **pub/ukstu/flair_form**.

Applicants requiring more than one run should not expect to be scheduled on consecutive lunations.

An observer is expected to go out to the UK Schmidt Telescope to assist with the observing and the daily set-up procedures (mainly fibring up). A second observer might be necessary if both plate holders are to be used on the same night. Given the heavy survey demand on the telescope it is possible that in exceptionally good seeing conditions the observer might be expected to give up one night to photography, in which case every effort would be made to extend the FLAIR run by one or two nights.

Mike Read, ROE, and Quentin Parker, AAO

lpinfo

Telescope News

WHT Technical downtime on the WHT has continued at a level of about 4%, and the winter has so far been very mild, with only 23% of WHT time lost to bad weather between September and January.

WHT infrared camera (WHIRCAM) and MARTINI commissioning runs are taking place in February and June. The three-mirror infrared derotator for GHRIL will be shipped to La Palma in April for final alignment in May. The chassis has already been aligned with the telescope.

ISIS will be dismantled early in April for an overhaul, to include the recoating of some optical components. It will be reassembled in May.

The UES autoguider software has been giving cause for concern for some months; no single version of the software can be used for both slit and offset guiding, and it is not possible, for example, to offset-guide while retaining a view of the slit. Remedial work is in progress.

The DIMM seeing monitor is now installed on its tower outside the WHT and logs a measurement every two minutes. Comparisons are under way with the seeing recorded by the Cassegrain autoguider.

INT The telescope has generally been performing well over the last three months, with loss of telescope time due to technical problems running at about 3.5%. However, the FOS CCD has failed irreversibly and is unlikely to be available for Semester 95B. Various options are being considered for a replacement.

There is now a complete document describing the TEK3 chip. There are two Ag red collimators for IDS on offer, and the efficiency curves of all collimators have been re-determined. Tests of data transfer between the ICS Perkin Elmer and the Sparc have started and they have been successful for a limited number of frames so far. Work continues.

Shack-Hartmann tests were performed at prime focus in December, with a load equivalent to that expected with the four-chip camera. Analysis of the observations is under way. The image was found to move in the east-west direction when the Cassegrain rotator was rotated. Distortion of the mirror cell is suspected, and the amplitude, 4 arcseconds, is consistent with the motion of the centre of rotation when observed at Cassegrain.

Small irregularities found in the dome rail, left over from the last grinding session, will be smoothed in May.

JKT The JKT has been performing well over the past three months with little downtime. The main problems have involved the data tape writing process and an incident of surface contamination of the TEK4 CCD. The TEK4 CCD has now been fully commissioned and is released for normal common-user observing.

LPINFO Transfers to World-Wide Web

As announced in *Spectrum* No 3, a wide range of information and documentation, including most of the User Manuals, has been made available to users of the World-Wide Web, and can therefore be accessed by appropriate information browsers such as *Mosaic* and *lynx*.

As well as entries for the telescopes and instrumentation, there is information on applying for time, calibration, signal-to-noise, the guide star server, the data archive, the APM sky catalogues and weather information and maps. All the information previously stored in the VAX-based system LPINFO has now been transferred, and this will consequently no longer be maintained.

Note, however, that the URL of the Cambridge World-Wide Web server has changed. The main Cambridge home page is now **http://www.ast.cam.ac.uk/** and the ING information pages are **http://www.ast.cam.ac.uk/~lpinfo/**.

Service Nights, Semester 95A

Part or all of the following nights are available for the service scheme on the ING telescopes, subject to schedule changes: D means dark; G, grey and B, bright nights.

WHT	ISIS/FOS/ Aux port (imaging)	March 1 (D), 10 (D), 13 (D), April 2 (D), June 2 (G), 3 (G), July 6 (G), July 19 (G), 27 (D).
	ISIS/FOS/ UES	March 14 (B), 17 (B), 18 (B), June 15 (B).
	UES	April 8 (B), 9 (B), 17 (B), 19 (B), May 4(G), 5(G).
	TAURUS (F-P)/ UES	May 9 (B), 12 (B), 16 (B).
	LDSS/UES	May 3 (G), May 24 (D).
INT	IDS/FOS	March 3 (D), 10 (B), May 2 (D), 11 (B), 14 (B), June 7 (B), 12 (B), 25 (D), July 2 (D), July 3 (G), 19 (G), 27 (D), 31 (D).
	Prime focus (imaging)	March 20 (B), April 8 (B), May 19 (G), June 5 (G), 6 (B).
JKT	CCD imaging	March 9 (B), 10 (B), 26 (D), April 7 (G), 8 (B), 24 (D), May 9 (B), 13 (B), June 10 (B), 11 (B), 25 (D).

Service requests should be for not more than 3 hours, including calibration.

All service applications should be mailed to **service@ast.cam.ac.uk**.

Status of service observations for all three telescopes and the service form are held on the Cambridge Sun cluster in the directory **/data/ftp/service** (when accessed locally). They can be obtained by anonymous ftp from (**ftp.ast.cam.ac.uk**) where they appear in the directory **/service**.

La Bajada

The quinquennial La Palma festival *La Bajada de la Virgen* will take place from July 2 to August 5 this year. Travel to and from the island is expected to be very difficult from the middle of June onwards and observers scheduled during this period are advised to make their arrangements as early as possible.

ING instrument sensitivities/SIGNAL program

A summary of known ING instrument sensitivities was published by Clegg *et al* in *Gemini* No 35, p 16. Measurements made since then are summarised below. The numbers given for spectroscopy are above-atmosphere apparent magnitudes which yield 1 photon/second/Å for a wide-slit observation made at the zenith.

WHT ISIS with the 158 lines/mm gratings and the TEK1 (blue arm) or TEK2 (red arm) CCDs (René Rutten, 17 May, 21 October 1994)

Wavelength	3500	4000	4500	5000	5500	6000	6500	7000	7500	8000	8500	9000
AB mag (blue arm)	16.9	17.8	17.6	17.5	17.3	17.1	16.8	16.3	15.7	15.3	15.3	15.4
AB mag (red arm)	12.5	16.3	17.1	17.4	17.7	17.9	17.7	17.6	17.4	16.9	16.5	16.1

WHT UES with the 79 lines/mm grating and the TEK1 CCD and IPCS (Max Pettini, 6 August 1993, see *Gemini* No 42, p 26)

Wavelength	3500	3750	4000	4500	5000	5500	6000	6500	7000	7500	8000	8500
AB mag (TEK1)	16.3	16.8	17.0	17.0	17.0	17.0	17.0	16.9	16.7	16.4	16.0	15.5
AB mag (IPCS)	14.6		15.1	14.9	14.7	14.3						

WHT LDSS with the TEK1 CCD (Dave Carter, 3 April 1994)

Wavelength	3600	3800	4000	4500	5000	5500	6000	6500	7000
AB mag (Med-*R* grism)				17.4	18.1	18.6	18.6	18.5	18.2
AB mag (Med-*B* grism)		17.1	17.8	18.4	18.5	18.6	18.5	18.3	17.9
AB mag (High-res. grism)	15.9	17.0	17.9	18.1	18.1	18.0			

INT IDS 235-mm camera with the Ag Red collimator, R300V grating, EEV5 CCD and with the Al Wide collimator, R150V grating and TEK3 CCD (Emilios Harlaftis, 28 November 1994, 19 January 1995)

Wavelength	3330	3500	4040	4520	5000	5480	6040	6520	7000	7480	8090	9080	9560
AB mag (EEV5 CCD)		13.4	14.3	14.6	15.0	15.4	15.5	15.5	15.6	14.7	14.0		
AB mag (TEK3 CCD)	13.0	13.8	15.8	16.1	16.1	16.0	15.9	15.8	15.8	15.5	15.0	14.2	13.6

The throughput of the IDS 500-mm camera has been measured only at 6700 Å; it is similar to that of the 235-mm camera. INT FOS (Emilios Harlaftis, 2 February 1994)

Wavelength	3500	4000	4500	5000	5500	6000	6500	7000	7500	8000	8500	9000	9500
AB magnitude	13.6	15.7	15.7	15.8	15.8	16.4	16.7	16.9	16.8	15.9	15.9	15.2	14.2

Response curves for the different CCDs available at the ING were given in *Spectrum* No 1, p 12.

Sensitivities for imaging through the Harris filters (response curves in *La Palma Technical Note 96*) have been determined for JKT f/15 with the TEK4 CCD (Reynier Peletier, 1 August 1994), INT prime focus with the TEK3 CCD (Reynier Peletier, 15 – 20 July 1994) and the newly-commissioned WHT prime focus with the TEK2 CCD (Dave Carter, Terry Bridges, Janet Sinclair, 25 – 30 April 1994). The numbers given are above-atmosphere apparent magnitudes which yield 1 detected photon/second at the zenith.

Band	*U*	*B*	*V*	*R*	*I*
JKT f/15	21.0	23.1	23.3	23.5	23.0
INT prime-focus	23.1	25.3	25.3	25.4	24.7
WHT prime-focus	24.1	26.2	26.4	26.5	26.0

Sensitivities have now been measured (for at least some wavelengths) for all common-user instruments except WHT TAURUS (Fabry-Perot), the JKT Richardson-Brealey spectrograph, and imaging with WHT LDSS or TAURUS f/4. The ratios between mean measured instrumental throughputs, and those predicted on the basis of estimated or measured efficiencies of individual optical components (*eg* mirrors, filters, gratings) are given in the table below, for representative wavebands.

	U	*B*	*V*	*R*	*I*
WHT ISIS	0.9	0.6	0.7	0.8	0.4
WHT FOS			0.8	0.7	0.8
WHT UES	0.9	0.5	0.6	0.5	0.6
WHT LDSS (spectroscopy)	1.7	0.7	0.7	0.7	
INT IDS 235	0.4	0.4	0.5	0.4	0.6
INT FOS	0.3	0.5	0.6	0.8	0.8
WHT prime-focus imaging	0.7	0.6	0.8	0.6	1.0
WHT aux-port imaging		0.9		0.6	
WHT TAURUS f/2 imaging		0.7	1.0	0.7	0.9
INT prime-focus imaging	0.9	0.8	0.8	0.6	0.9
JKT f/15 imaging	0.9	0.7	0.9	0.9	1.0

The small scatter of values for each instrument confirms that the error in measuring the instrumental sensitivities is typically 10 – 20%. The INT IDS 235 mm camera has a throughput much less than that predicted; its optical surfaces are visibly dirty, and a major overhaul of IDS is planned for September 1995.

SIGNAL

The measured sensitivities are incorporated in a Fortran program SIGNAL, which can be used to predict the number of object and sky photons which will be detected during an exposure with one of the common-user instruments of the Isaac Newton Group on La Palma, as a function of apparent magnitude, wavelength band, diffraction grating, detector *etc*. The program was described in *Gemini* No 35, p 20. The current version (which differs from the 1992 version in using empirical instrument sensitivities rather than theoretical predictions) may be obtained by email from the author, or by anonymous ftp via the ING information page on the Cambridge server **ftp://ftp.ast.cam.ac.uk/pub/lpinfo/signal/**. The program can be used before observing to estimate the exposure time needed for a particular experiment, and at the telescope to check that the expected number of photons (counts × gain) is arriving at the CCD. With thanks to the ING and RGO support astronomers for providing reduced throughput data, and for comments.

Chris Benn, ING La Palma

NOT

Within an informal agreement for the exchange of telescope time, members of the PATT community are encouraged to apply for observing time on the 2.56m Nordic Optical Telescope (NOT) at the Observatorio del Roque de los Muchachos. Applications are currently invited for the allocation period that runs from October 1995 to March 1996. The deadline for this period will be near the middle of May. Proposal forms and further details can be obtained from the Director, Nordic Optical Telescope SA, Lund Observatory, Box 43, S-221 00 Lund, Sweden, e-mail **not@astro.lu.se**.

A Message from the ING Scheduler

In order to arrive at an optimum schedule (and make my task a little easier), I would like to ask all PATT (and CAT) astronomers who are applying for telescope time on the ING telescopes in the next round of applications to please:

list the RAs and Decs of *all* their targets, rather than just a sample. Even the full range of RAs and Decs would be a help;

give full reasons for impossible dates. In particular, where there is only a single object or field, I would urge the applicant to check whether the position of the Moon is going to be a problem and if so, list such dates. I do not always have time to do these calculations myself;

try and tell me of any possible clashes you are likely to have with other telescope runs and/or instruments;

fill in the instrument scheduling form (correctly).

I believe that the AAT scheduler echoes some of these sentiments as well! I thank you and look forward to a trouble-free schedule next time.

Bill Martin, RGO

The Non-thermal Emission in M87

The emission from radio galaxies generally originates from three components, the nucleus, one or two jets, and some radio lobes, which often contain knots and hotspots. It is generally thought that the emission from these components is synchrotron radiation, due to energy losses from relativistic electrons in a magnetic field. In some galaxies this emission is also seen at optical wavelengths, in the jets and sometimes in the hotspot. M87, the central galaxy in Virgo, is the closest giant elliptical showing this phenomenon in the optical. It has a bright optical jet, and recently (for example Stiavelli *et al* 1992, *Nature*, **354**, 132, hereinafter S92) the optical counterpart has been detected of a hotspot in the (eastern) lobe on the opposite side ofthe jet as seen from the nucleus. From energy and lifetime arguments the presence of a counterjet in M87 has been inferred from this hotspot.

Non-thermal components of emission from M87 are picked out by IRCAM3 K-band imaging.

The spectral index of optical jets is usually determined between radio and optical wavelengths. It varies from one galaxy to another, and also within the jet. The further one goes from the nucleus, the steeper the spectral index gets. Since in *V–K* parts of the jet are redder than the stars, one should be able to better separate the thermal and non-thermal component in M87 in the near-infrared than in the optical. We decided to try and see whether IRCAM3 was stable enough to do this.

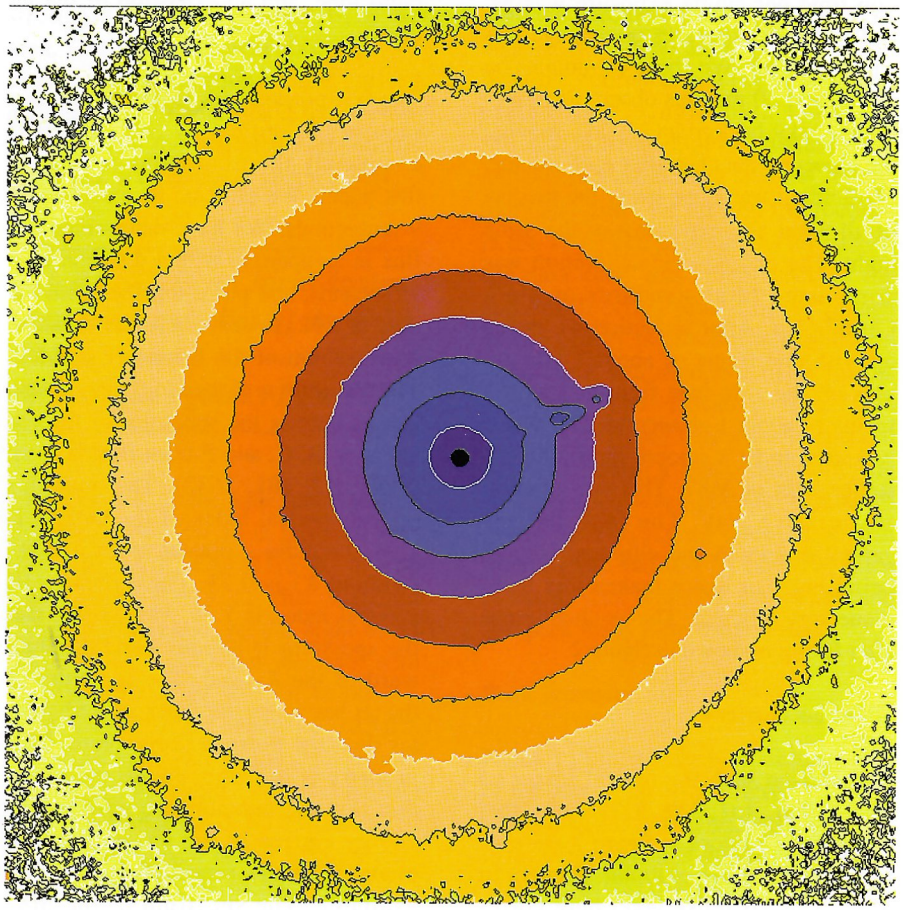

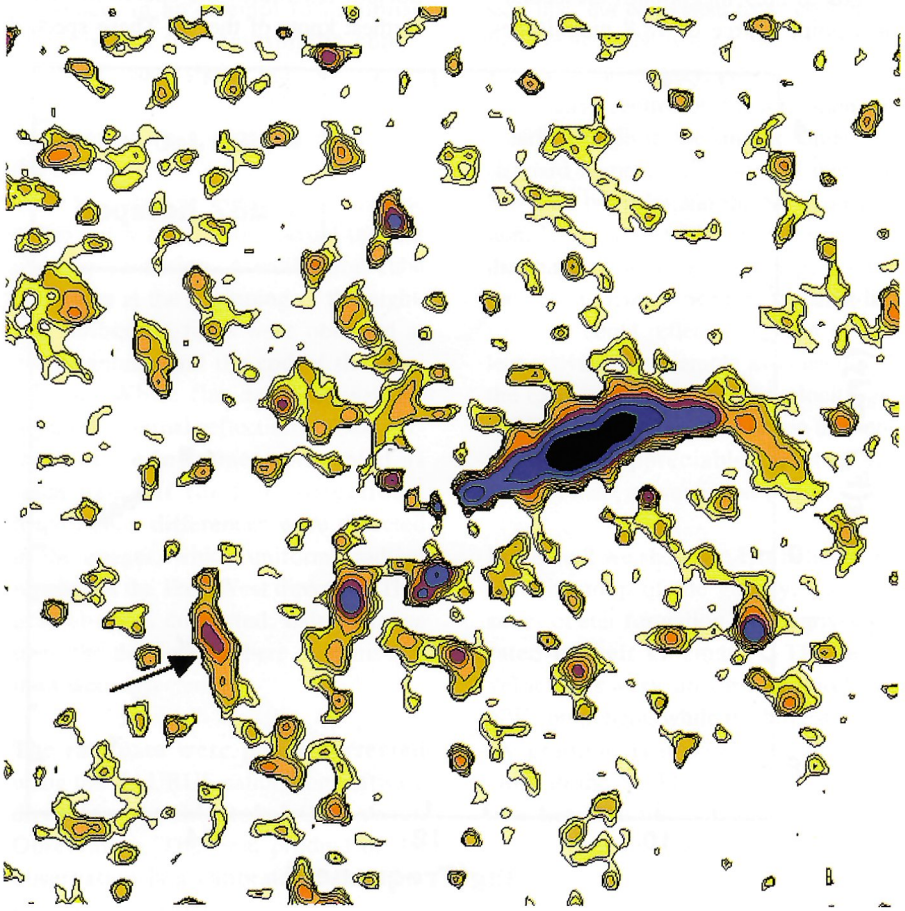

Fig. 1 (top) – Contour and grey scale map of M87 in K. The size of the image equals 106 arcseconds on the side. Given are contours from 13 to 20 magnitude arcseconds^{-2} with steps of 0.5 magnitude arcseconds^{-2}.

Fig. 2 (bottom) – Contour map in K of what is left after subtracting a symmetric model (see text). The image size is 89 arcseconds on the side. The hotspot is the large almost vertical feature on the left (east). Contours here are 16, 17, 18, 19, 19.5, 20, 20.5, 21, 21.5 and 22 magnitudes arcsecond^{-2}.

We observed M87 in the beginning of June 1994, in the *K*-band, using the new 256 × 256 InSb array. The integration time per single exposure was 3s, and every 20 exposures on average was written to disk. We spent 45 minutes on source and 30 minutes observing neighbouring sky background fields, moving the object on the chip after each minute. Flatfielding was done using the median of all night sky exposures of the same night. The photometric calibration was done using faint standards of Mark Casali's list. After reduction we ended up with one frame of about 2 arcminutes on the side (see figure 1) with a seeing of about 1 arcsecond. This frame was used to fit a smooth model for the stellar light of M87. This was done in an iterative way. The fact that the galaxy is smooth and elliptical without being boxy or disky makes this technique very efficient. The residual image after fitting is shown in figure 2.

Globular clusters

Comparison with the optical image of Keel (1988, *ApJ*, **329**, 532) shows that most of the sources in figure 2 are real. Most of them are globular clusters in M87. The 3σ noise level here corresponds to 20.9 magnitudes arcsecond^{-2} or a point source of 18.8 magnitudes.

Comparison with the 2 cm radio map of Biretta (see S92) shows two remarkable features, namely the hot spot in the east radio lobe, and an extension of the jet itself.

The hotspot appears to be larger than seen in the optical by S92, and fills completely the 6 cm radio contour in that paper. We estimate its extent to be 9 arcseconds. We have determined the flux in an aperture with a diameter of 4 arcseconds, and put it together with the data of S92, to see where the break in the spectrum of the hotspot would fall. The spectrum is plotted in figure 3. Also shown here is the spectrum of the jet, knots A, B, C, and F from Biretta *et al.* (1991, *AJ*, **101**, 1632). The optical – optical spectral index of the hotspot is 1.93, the radio – optical spectral index (without *K*) is 0.73. The optical – IR spectral index is 1.56. This shows that the spectrum is already bending blueward of the *K*-band. The spectrum of the jet has a spectral index of 0.65, flatter than the hotspot everywhere. This property is probably connected to the fact that the hotspots are powered by energy carried in the jet; no detailed model for these processes is however available. The spectrum of the M87 hotspot resembles the spectrum of the furthest knots of the jet. These spectral indices for the hotspot are consistent with other hotspots, *eg* those of 3C33 S or Pic A. Preliminary results from detailed synchrotron fits to the jet and hotspot spectra including the new IR fluxes indicate that the apparent steepening is probably due to the upper energy cut off coming progressively into the optical region.

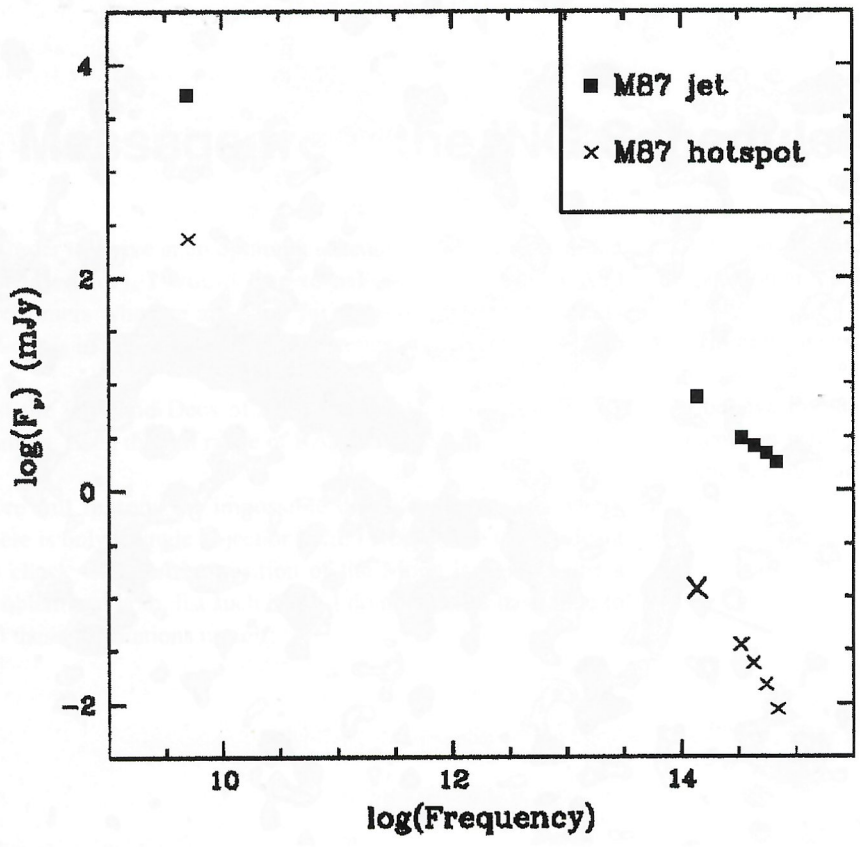

Fig. 3 – Spectrum of both jet and hotspot from radio to optical.

Lowest contour

The jet on the other hand seems to continue a long way from the centre. The lowest contour drawn on figure 2 corresponds to $K = 22$ magnitudes arcsecond^{-2}. For a spectrum as steep as that of the hotspot this would correspond to $V = 26.1$ magnitudes arcsecond^{-2}, or about 4.5 magnitudes below the level of the sky. Optical – IR spectral index measurements here should in principle be possible. It appears again that all features of the jet that appear in radio are also seen in the optical or the near-infrared. This could mean that many more radio jets could be discovered in the optical or in the near IR as well in the future.

Just before finishing this paper we found that similar kind of work had been done by Neumann *et al* using the MAGIC camera at Calar Alto. They don't go as deep as us, but do confirm that the hotspot in *K* is much larger than in the optical. They also claim to have detected a new feature at the southern limb of the eastern lobe, which they call η. With our new, higher signal-to-noise data we find that the appearance of the infrared light at that position is very different from the shape at 6 cm, so that we think that their detection corresponds more probably to two globular clusters or a galaxy than to non-thermal emission. We have also taken some exposures of this galaxy in *L'*, and apart from the nucleus the most prominent feature here is the jet. We conclude that IRCAM3 is a very stable and efficient instrument. We have not encountered any problems that caused a fundamental limit to the depth of the images. The large wavelength range of the detector makes IRCAM3 an ideal instrument to study such problems as the spectral energy distribution of synchrotron jets.

R F Peletier, ING, M Stiavelli,
Scuola Normale Superiore, Pisa

TAURUS-2 Observations of I Zw 18

Blue compact galaxies are characterised by an optical spectrum resembling that of an extragalactic giant HII region. Their deficiency in the abundance of heavy elements, together with the fact that they are also rich in neutral gas, suggests that they are young objects, probably experiencing the first burst of star formation. Studying the kinematics and dynamics of these objects can provide us with clues about the mechanism which triggers star formation, and about the processes that influence their chemical evolution, for example the change in the metal contents due to the effect of stellar winds or supernovae explosions.

Studies with high spatial and spectral resolution over the complete area of the object allow us to study the fine scale structure of the velocity field and to understand the physical process that regulates the dynamics of the gas. Imaging spectroscopy provides an ideal method, combining high spectral resolution with multiplexing spatial abilities that allow coverage of a complete galaxy, avoiding the undersampling problems associated with long-slit spectroscopy. The Observatorio del Roque de los Muchachos on La Palma provides an ideal instrument for this type of study, thanks to the availability of TAURUS-2, a Fabry-Perot imaging spectrograph designed to obtain velocity fields of extended objects such as giant HII regions, supernovae remnants and galaxies. Combined with the excellent seeing at the observatory, the power of imaging spectroscopy brings us new insights into the physics of these objects.

Preliminary results

To illustrate our work, we present here preliminary results of the prototype HII galaxy I Zw 18. It has one of the lowest metal abundances known (1/50 of solar abundance), and is hence a crucial object for estimating the primordial abundance of helium. Recent studies suggest that no more than one burst of massive star formation has occurred in the past. Located at a distance of 10 Mpc, it is formed by two giant nebulae, separated by 5.8 arcseconds. The optical component coincides roughly with the strongest concentration of HI in the area. Our main aim was to obtain the kinematic information of the ionised material, and to understand the interaction between the different components of the gas in a relatively young object.

TAURUS-2 is an ideal instrument for the studies of the physical processes at work in the blue compact galaxy I Zw 18.

Observations of the kinematics of the ionised gas of I Zw 18 in Hα were carried out with TAURUS-2, at the Cassegrain focus of the William Herschel Telescope, on the night of 11 May 1992. The f/4 focus was used with the EEV3 CCD as detector (1 pixel = 0.56 arcseconds), and the 125 μm etalon, providing a free spectral range of 17 Å at the wavelength of Hα. The data cube was composed of 60 frames of 330 × 330 pixels, each frame with an integration time of 100 seconds. The scan sequence was made in a random sequence, in an attempt to minimise variations in the atmospheric conditions; the mean seeing was 1.7 arcseconds. A top-flat filter of 15 Å FWHM was used at the appropriate redshift of the object (6577 Å for 750 km s^{-1}), in order to isolate an order of interference of the Fabry-Perot and to avoid the risk of order confusion. A calibration cube was taken at the beginning of the night, and calibration rings were obtained at the beginning and the end of the integration. While flat data cubes were obtained, internal reflections on the surfaces of the instrument prevented us from using it for flat corrections. Illumination differences were detected in the images, with a uniform gradient running in the East-West direction. That gradient was corrected, using planes from the data cube where no emission lines were detected.

The raw data were phase-corrected using the TAURUS calibration software developed at the Royal Greenwich Observatory. The final product of the observation is a calibrated data cube, two axes in spatial coordinates, and the third the wavelength scale. New tools of analysis have been developed to manipulate the enormous amount of data generated by a single data cube (20 Mbytes) in an attempt to automatise the arduous process of data analysis. In this particular case, we applied the routines in the TAUFITS package. As a first step the data cube was compressed in the spectral direction producing an image of the object in the Balmer emission line, which was used as a mask for the program. The velocity field was obtained by fitting Gaussians to spectral lines, assuming a flat continuum. The line profiles were produced at each point by extracting spectra within square areas, defined by boxes of three pixels in size. Velocity, line width and line peak maps were then created.

Peak intensity

Figure 1 illustrates the peak intensity map of the galaxy (in all the figures, north is top, and east is left). The image is similar to the compression of the data cube in the spectral direction which created the image of the object in the Balmer emission line, but equivalent to a "continuum free" image. The two prominent condensations in the galaxy, which denote the most active centres of star formation, are clearly visible in the image. Under the standard nomenclature, we call them the NW (the brighter) and the SE condensation. Note that the NW condensation has the shape of an incomplete ring, 3.3 arcseconds in diameter. While the shell-like structure could reflect some sort of violent activity, for example associated with the existence of very high velocity gas (FWZI 3600 km s^{-1}) detected on the knot, there is no appreciable effect on the velocity map, as we discuss below.

In figure 2 we show the Hα heliocentric velocity map of the galaxy. The two zones of star formation are clearly separated in their kinematics. The radial velocity is very uniform through the NW component, while the largest velocity gradient is observed in the zone close to the SE knot. It is important to note here that the global velocity structure is very similar to that observed in HI. From a gradient velocity map, we find maximum values of 7 km s^{-1} arc-

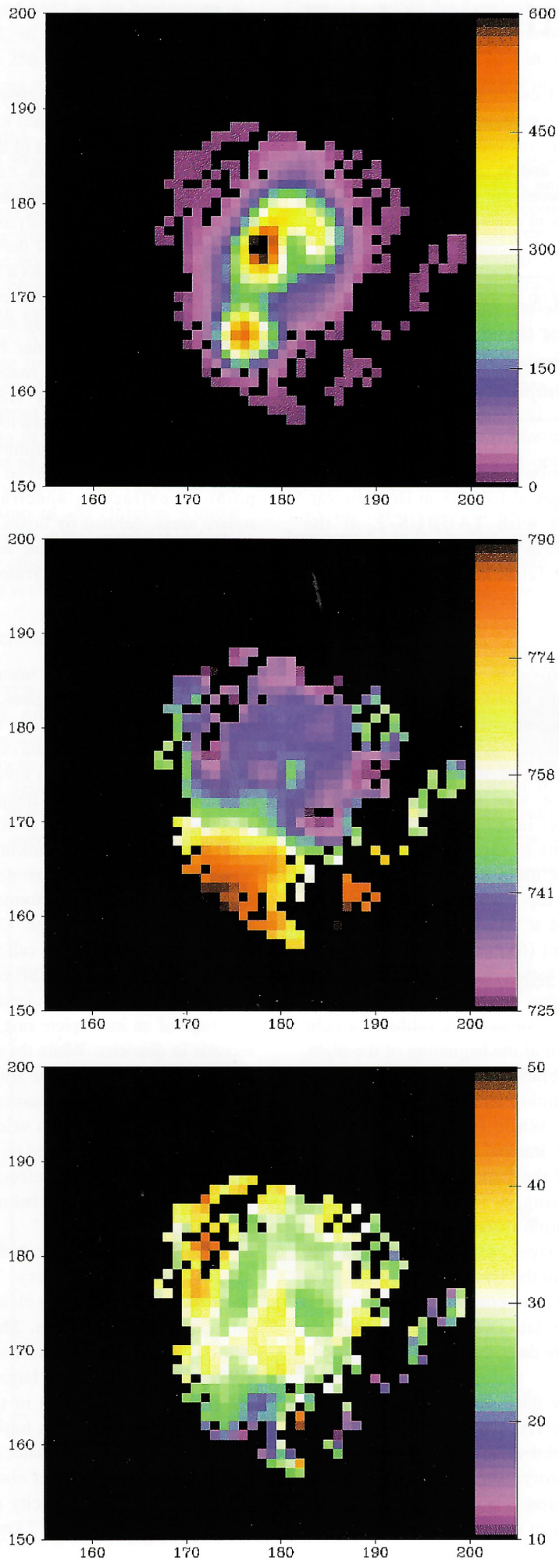

Fig. 1 (top) – Intensity peak map of I Zw 18. The map represents the maximum intensity of the Gaussian fit above the background for Hα.
Fig. 2 (middle) – Velocity map of I Zw 18 in Hα, in units of km s^{-1}.
Fig. 3 (bottom) – Velocity dispersion (σ) map of I Zw 18, in units of km s^{-1}. The map has been corrected by instrumental broadening.

second^{-1}. The existence of two clearly differentiated kinematic structures is also seen in the velocity histogram, which shows a bimodal distribution, one centred around ≈ 740 km s^{-1}, and the second one around ≈ 775 km s^{-1}.

A critical assumption to calculate the mass of the galaxy is the origin of the velocity field. Previous estimates for the mass assumed that the field was due to circular rotation. It is clear that this is hard to reconcile with the velocity map observed. Both areas of star formation show different properties. A more likely model is that the galaxy is the result of a merger of two (or more) clouds of gas, each with their own velocity field. Our results confirm recent findings by Skillman and Kennicutt, via long-slit spectroscopy, but now we have a complete map of the kinematics of the gas available to support their conclusions.

Velocity dispersion

The final figure is the velocity dispersion map (σ), after correction for the instrumental line width. Note how the shell structure of the NW knot can also be traced in the map (typical values are ≈ 25 km s^{-1}), while the most turbulent zone is the area between the knots. If we take the typical sound velocity to be of order σ ≈ 7 km s (the velocity dispersion in one dimension) we see that most of the gas is in a state of supersonic turbulence, with values clustered around 28 km s^{-1}.

The aim of this article has been twofold. First, to discuss the dynamics of the ionised gas in a typical HII galaxy, and secondly, to show to the user community the power of two-dimensional spectroscopy in the analysis of the velocity field of extended objects.

We want to thank Steve Unger and all the staff at La Palma for the excellent support provided during the programme, and Jim Lewis at RGO for his help during the reduction and analysis of the data.

Héctor Castañeda, IAC/ING La Palma,
Oriol Fuentes-Masip, IAC

A Radio Galaxy at $z = 4.255$

In principle, radio galaxies are sufficiently luminous that they can be seen out to $z \sim 5$, and the properties of objects at such high redshifts are obviously of great astrophysical interest. Unfortunately, the geometry of the Universe, combined with a probable cut-off in the numbers of radio sources past a peak at $z \sim 2$ and the shape of the luminosity function, conspire to make $z > 3$ objects very rare, no matter what flux level is used to select a sample. Previous attempts to find high-redshift radio galaxies have searched for objects with extreme radio properties, and then observed these candidates spectroscopically. A particularly successful technique is to select candidates with a steep radio spectral index at $\gtrsim 100$ MHz. This approach led Chambers, Miley and van Breugel to the discovery of 4C41.17 at $z = 3.8$, which was until now the most distant galaxy known.

The most distant galaxy yet discovered has been found from WHT spectroscopy of radio sources selected at 38 MHz.

We have extended this strategy to samples selected at the much lower frequency of 38 MHz, using a survey by Rees. We selected various candidates from 970 8C radio sources covering about 0.2 steradians of sky. Our $z = 4.255$ candidate, 8C1435+635 was found in a sample selected on the basis of highly-curved spectra, which flattened or turned-over at low frequencies.

Following our candidate selection, we obtained maps at 1.5 GHz using the VLA in A-array. These maps gave positions sufficiently accurate to enable spectroscopy of the smaller (< 15 arcsecond) sources without imaging.

Optical spectra

Our candidate high-z sources are optically very faint, which makes direct acquisition for spectroscopy difficult. Fortunately, the accurate source positions from the VLA maps and the pre-

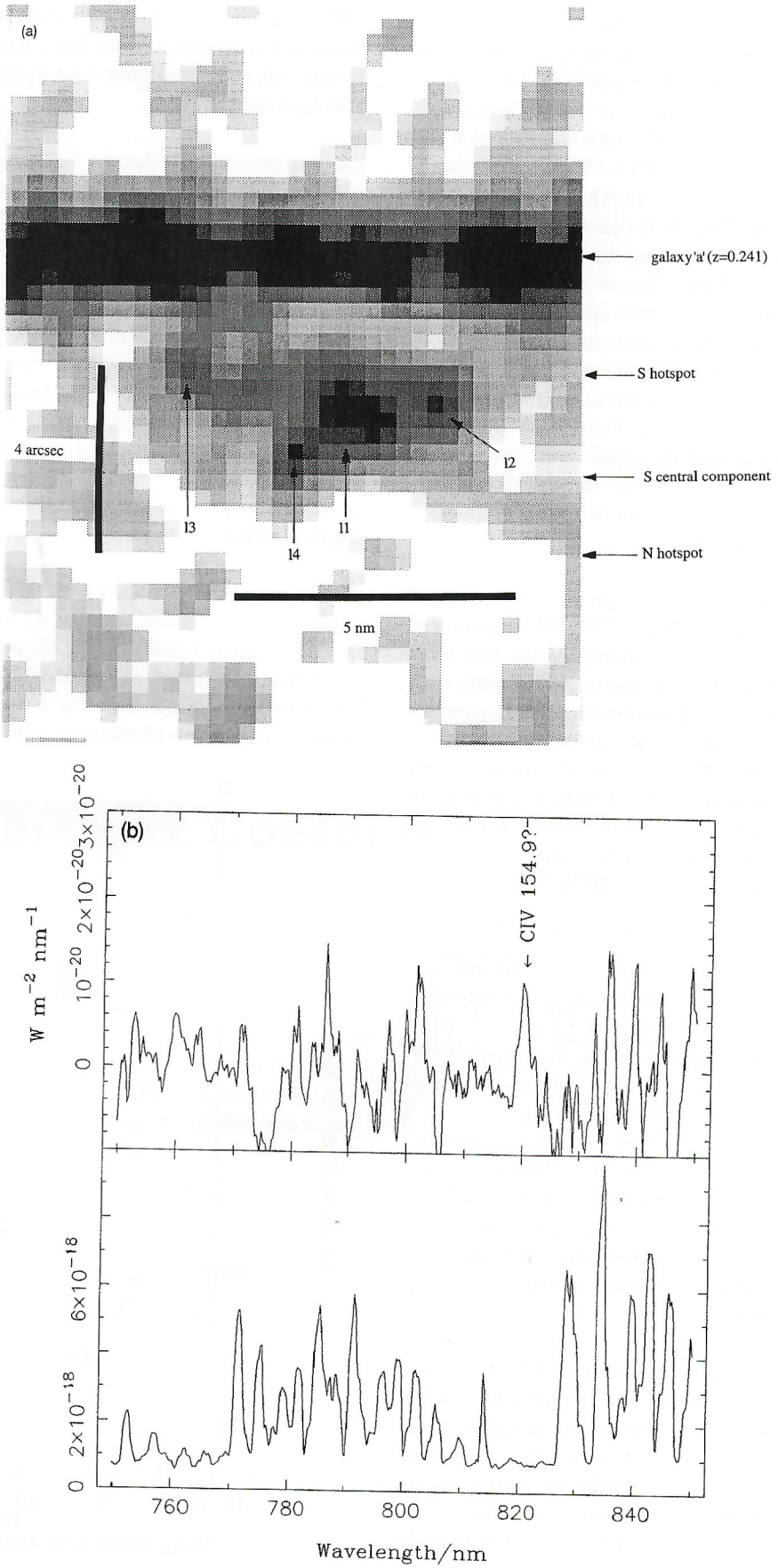

Fig. 1 – The optical spectrum of 8C1435+635: (a) greyscale of the Lyα line showing the unusual spatial and velocity structure; (b) the region around the CIV 1549 candidate with the sky spectrum shown below.

cise pointing of the WHT mean that it is possible to position the objects on the slit by offsetting from a nearby star, without seeing the object on the acquisition TV. Such "blind spectroscopy" was carried out for our sample during three runs using ISIS on the WHT.

The runs in 1993 June and 1993 August were made with a 540 nm dichroic in place and the TEK1 CCD in the blue arm. The 1994 February observations were made using the red arm only, and no dichroic. The red arm detector on all three runs was the EEV3 CCD. Conditions in June were non-photometric but transparency was good, and conditions in August and February were very good. We observed 8C1435+635 for a total of 12600s, and chose to set the slit at two different position angles to provide spectra of several neighbouring galaxies.

Analysis of the spectra was performed using the IRAF TWODSPEC package, and involved subtracting the bias level from the raw spectra which were then flat-fielded and transformed to straighten both the sky lines and the object trace. The background was subtracted by fitting a 6 – 8 order polynomial to each column. Flux calibration was carried out using the standards BD+284211, BD+404032 and GRW705824.

The spectra show a resolved, spatially extended emission line centred on 639.0 nm, with a flux of $1.6 \pm 0.3 \times 10^{-19}$ Wm^{-2} (figure 1). The line has a FWHM of 1800 kms^{-1} and consists of several components (l1 to l4 in figure 1) which have velocities between −1500 and +700 kms^{-1} relative to the main component, and angular separations up to 2 arcseconds. A further line is detected at 820.5 nm in both the 1993 and 1994 spectra, with a flux of $3.4 \pm 0.8 \times 10^{-20}$ Wm^{-2}.

We have chosen to identify these lines with Lyα at $z = 4.255$ and CIV 154.9 at $z = 4.297$, which means that CIV is redshifted by 2400 kms^{-1} relative to Lyα. Although this velocity shift is large, shifts of ~ 1000 kms^{-1} are not uncommon between Lyα and other lines in these objects.

We have considered the possibility of other identifications for the lines. The next closest ratio is C III]190.9/[Ne IV]242.4, in which case the [NeIV] line is redshifted by 3300 kms^{-1} with respect to the C III]. We consider this unlikely though as no line is detected in the blue arm spectra, whereas we would expect to see both Lyα and C IV 154.9.

Another possibility is that the C IV line is an artifact. If this were the case the most likely identification for the 639.0 nm line would be [O II]372.7 at $z = 0.71$, the only other high equivalent width line apart from Lyα which is frequently found to be spatially extended. However, in this case we would expect to see [O III]500.7 in the spectrum at a similar flux level, whereas in fact no candidate is detected to a 3σ limit of 1.1×10^{-20} Wm^{-2}.

Optical images

Direct images in the *R* and *I* bands were obtained using the IAC camera on the Nordic Optical Telescope (NOT) and were bias-subtracted, flat-fielded and calibrated in the usual way. The *I* band image was taken in photometric conditions, and the *R* band in non-photometric conditions, but in fair transparency.

The *R* band image of the galaxy and surrounding field are shown in figure 2. The radio galaxy is detected at 4σ with $R \approx 24.1$ in a 3 arcsecond diameter aperture and appears to be extended along the radio axis towards the southern hotspot seen in Merlin and VLA radio maps. Most of the emission in this filter is probably from the Lyα line, which lies in the *R* band. The galaxy is undetected in *I* to a 3σ limit of 23.3.

Discussion

The observed radio luminosity of 8C1435+635 ($L_{151} = 6.5 \times 10^{27} h^{-2}$ $WHz^{-1}sr^{-1}$) places it at the very top end of the radio luminosity function. However, there are several nearby field galaxies seen in figure 2 and these suggest the possibility that gravitational amplification is taking place. The likely amount of amplification depends on whether the three galaxies at $z \approx 0.23$ are members of a cluster perhaps centred on 'b', or just represent a small group. We can, however, make a crude

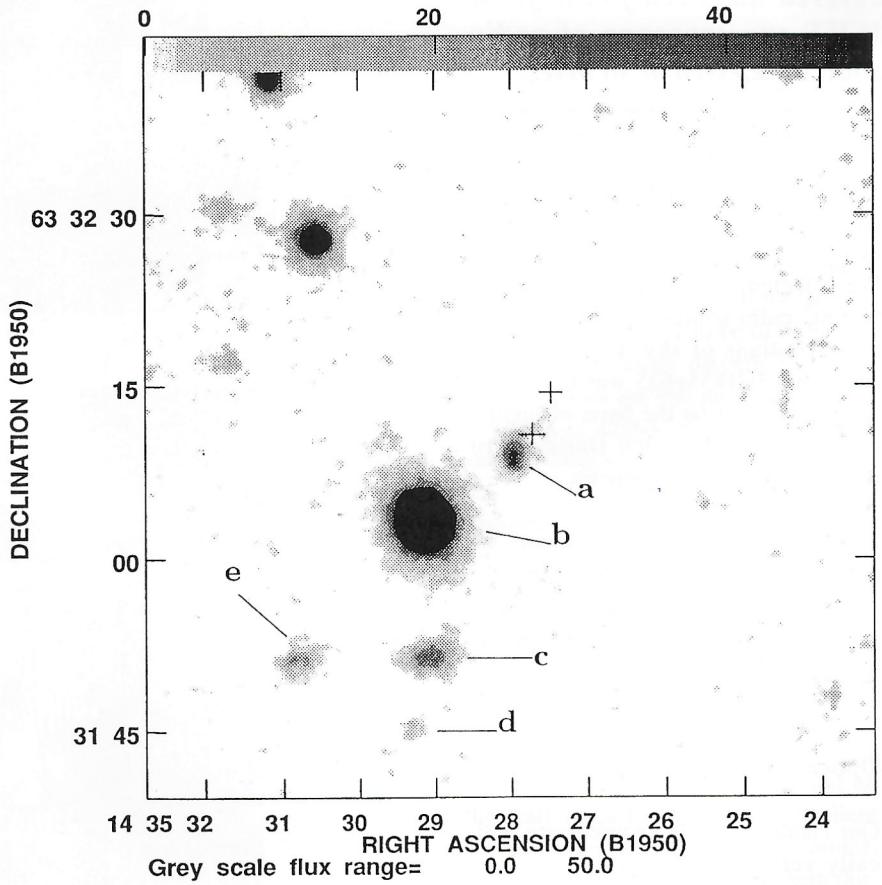

Fig. 2 – The R-band image, showing the identification and surrounding galaxies. The radio hotspots are marked with crosses. The galaxies a, b and c have $z \simeq 0.23$, and galaxies d and e have $z \simeq 0.36$.

estimate of the amount of amplification if we use the fact that the image does not appear to be very distorted. With reasonable models of the lens, we expect that the amplification factor would be $\lesssim 3$. Even if we assume that the apparent radio flux of this source has been amplified by a factor of three, the unamplified flux would still lie above the flux limit of most other surveys for ultra high-z galaxies.

The high luminosity of 8C1435+635 suggests that the evolution of radio-loud AGN at high redshift may be similar to that of radio-quiet quasars. Investigations of radio-quiet quasars have shown that the space-density of the most luminous quasars at $z \gtrsim 3$ decreases more slowly with increasing redshift than that of lower luminosity quasars. This effect means that most of the known $z > 4$ quasars are at the top end of the luminosity function. If radio-loud AGN are similar we would expect those found at high redshift to have high luminosities.

The Lyα flux is low for such a radio-bright object, lying about an order of magnitude below McCarthy's [O II] luminosity/radio luminosity correlation (*Annual Review of Astronomy and Astrophysics* 1993, **31**, 639), assuming a Lyα/[O II]372.7 ratio of 5. Unless the optical flux is being extinguished by dust in the foreground cluster, this may indicate that Lyα is suffering resonant scattering or absorption by H I or dust, and/or that the emission line strength in this object is anomalously weak, perhaps due to dust extinction towards the emission-line region.

If either or both of these is a general property of $z > 4$ galaxies, it may make finding more examples challenging, particularly if lensing really is important for 8C1435+635.

This work is part of a long term multi-wavelength project to find and observe high-redshift radio galaxies, and involves a cast of thousands, including: George Miley, Malcolm Bremer, Rob van Ojik and Huub Röttgering (Sterrewacht Leiden, Leiden); Steve Rawlings (Department of Physics, Oxford); Richard Saunders, Guy Pooley, Garret Cotter and Peter Warner (MRAO, Cambridge); Mark Dickinson (STSCI, Baltimore); Simon Garrington (Nuffield Radio Astronomy Laboratories, Jodrell Bank).

Steve Maddox, RGO,
Mark Lacy, Oxford

The 36th Herstmonceux Conference

The 36th Herstmonceux Conference, entitled "Gravitational Dynamics" will be held in Cambridge from 7 – 11 August 1995. The conference is being held in honour of Donald Lynden-Bell's 60th birthday, and the topics covered will range widely, reflecting Donald's exceptionally broad spectrum of research interests. They will include disks, stellar systems, the Local Group, large scale structure and motions, testing gravity and galaxy formation. Most of the conference will be taken up by invited talks, though a number of very short (5 minute, 1 transparency) contributions are being arranged. There will also be facilities for poster presentations.

The conference is jointly sponsored by the Institute of Astronomy and the Royal Greenwich Observatory; it is partly funded by the EC. The organisers are Ofer Lahav (IoA) and Roberto Terlevich (RGO). Further details are available from **gravity@ast.cam.ac.uk**.

The Episodic Outflow in L1448

L1448 is one of the most spectacular examples of an extremely-high-velocity molecular outflow from a young, low mass star. The outflow, first mapped with the IRAM 30 m telescope in CO J = 2–1 by Bachiller *et al*, is highly collimated though rather clumpy. Radial velocities approaching 70 km s^{-1} are measured in the outflow, and for symmetrically placed clumps on either side of the embedded source, L1448-mm. We have since observed the outflow in the H_2 v = 1-0 S(1) ro-vibrational line (a much-used diagnostic of low to intermediate velocity molecular shocks in outflows) at UKIRT and more recently with the MAGIC near-IR camera on the 2.2 m telescope in Calar Alto, Spain. The H_2 (plus continuum) image in figure 1 is of the northern, blue-shifted outflow lobe only. L1448-mm is marked with a cross. One clearly sees the strikingly curved morphology of the H_2 "jet", and the apparent superposition of two, and perhaps three bow shocks roughly equally spaced along the length of the flow (labelled A, E and H).

The spectroscopy

Echelle spectra have also been obtained in L1448 with CGS4 and the long camera, at eight slit positions in the northern, blue-shifted outflow lobe. The slits were aligned along the flow direction (p.a. = 118°), each slit being shifted by 2 arcseconds in R.A. Since the pixel scale along the slit is ~ 2 arcseconds, a very credible image of L1448 is obtained by summing the H_2 emission in each spectral image along the dispersion direction, and then aligning these image strips (in figure 2 north is at p.a. 28° in this image).

The spectral images at the eight slit positions are displayed in figure 3. No continuum emission is seen in these images, only H_2 v = 1-0 S(1) line emission. Of particular interest in these data are the very wide line profiles which extend out to −70 to −95 km s^{-1} (the systemic velocity is ~ 5 km s^{-1}). Like the CO, the shocked H_2 is all blue-shifted, in some cases out to extremely high velocities. However, because H_2 is thought to be dissociated in shocks with speeds in excess of ~ 50 km s^{-1}, the H_2 profiles can only be explained in terms of curved or bow-shaped shock geometries. Indeed, one sees that the widest H_2 line profiles are observed towards the proposed bow shocks, particularly knots A and E. (Note that the strips that comprise the image in figure 2 cover the same length along the slit as the images in figure 3. Consequently, by comparing each column in the image in figure 2 with the associated spectral image in figure 3 one can easily identify the position in the outflow of each spectrum.)

CGS4 echelle spectroscopy of the high velocity molecular outflow from L1448 shows a series of bow shocks probably resulting from episodic outbursts.

Bow shocks

The bottom feature in the spectral images 1 to 6 (in figure 3) corresponds to the bow shock labelled A. As we move from slit position 1 to 5 we move up the western wing and onto the apex of this bow shock. The H_2 velocity steadily increases as we approach the head of the bow. Moreover, the shape of the feature becomes more triangular. At slit positions 4 and 5 the profile is typical of a bow shock: the velocity at the head is 40 – 50 km s^{-1}, this being the radial component of the shock velocity, while a few arcseconds to the south the profiles widen and in fact become double peaked, at ~ 30 and ~ 80 km s^{-1}. The two peaks probably correspond to the foreground and background H_2 velocities in the wings of the bow shock shell. The spectroscopy and imaging together thus provide compelling evidence for the bow shock nature of knot A in the L1448 H_2 jet. Future modelling and interpretation should also shed light onto the flow velocity and orientation in this region. Similar broadening of the H_2 profile in the second potential bow shock, knot E, is also evident in these data.

In image 7 in figure 3 the bright, elongated feature near the centre of the image corresponds to knots B to D (figures 1 and 2) while in image 6 the central feature corresponds to knot E. The H_2 velocity clearly increases, from ~ 50 to ~ 60 km s^{-1}, along this ridge B – D, and peaks at about 70 km s^{-1} in knot E. We do not, however, interpret these data in terms of acceleration along the outflow. Instead, the velocity gradient is thought to be a feature of entrainment in the extended, eastern wing of the bow shock knot E. H_2 will be shocked and accelerated to high velocities (almost equal to the shock velocity) near the head of the bow shock E, while as we move farther south along this limb-brightened eastern wing the H_2 is accelerated to progressively lower velocities. A similar effect is observed in the western limb of the bow shock knot A (in spectral images 1 to 5) and in the spectral features corresponding to knots F, G and H (in the spectral images 5, 4 and 3 respectively), where these knots are thought to represent the eastern wing of a third bow shock, knot H. The data therefore strongly suggest that the L1448 outflow consists of a series of bow shocks equally spaced along the length of the flow. The bows themselves probably result from episodic, if not periodic, bursts of outflow activity, as envisaged in the models of *eg* Biro & Raga. We note that there is additional evidence of episodic flows in observations of other outflows from young, low mass stars (*eg* HH 111 and HH 212).

Acknowledgments

It is a pleasure to thank Colin Aspin for his support during the observing at UKIRT, and Mike Smith for discussions on H_2 in jets and bow shocks.

Chris Davis, Max-Planck-Institut für Astronomie, Heidelberg

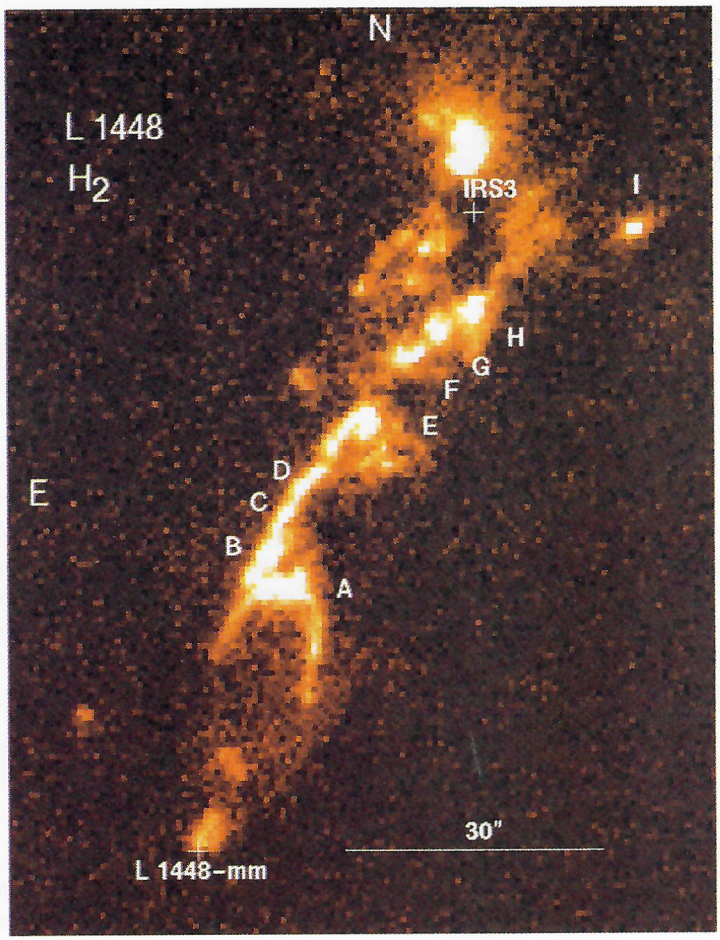

Fig. 1 – Narrow-band H_2 (+ continuum) image of the northern, blue-shifted lobe of the L1448 outflow. The flow is powered by the millimetre source L1448-mm. Individual knots in the flow are labelled. The unlabelled features to the north-east of the L1448-mm outflow are part of a second, conical outflow driven by IRS3.

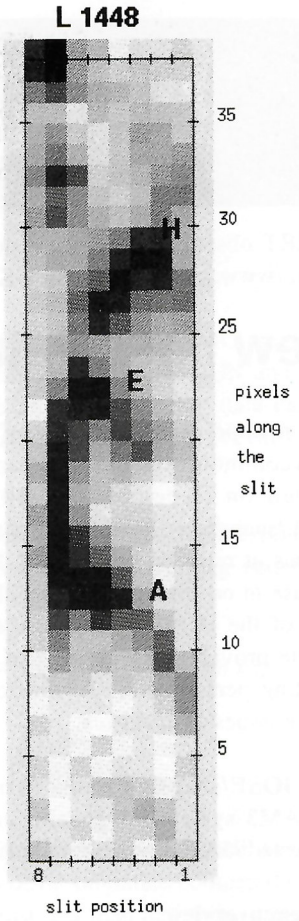

Fig. 2 – Composite image of the L1448-mm outflow constructed from the eight spectral images shown in figure 3. The eight columns correspond to the eight slit positions observed. North is at p.a. = 28°.

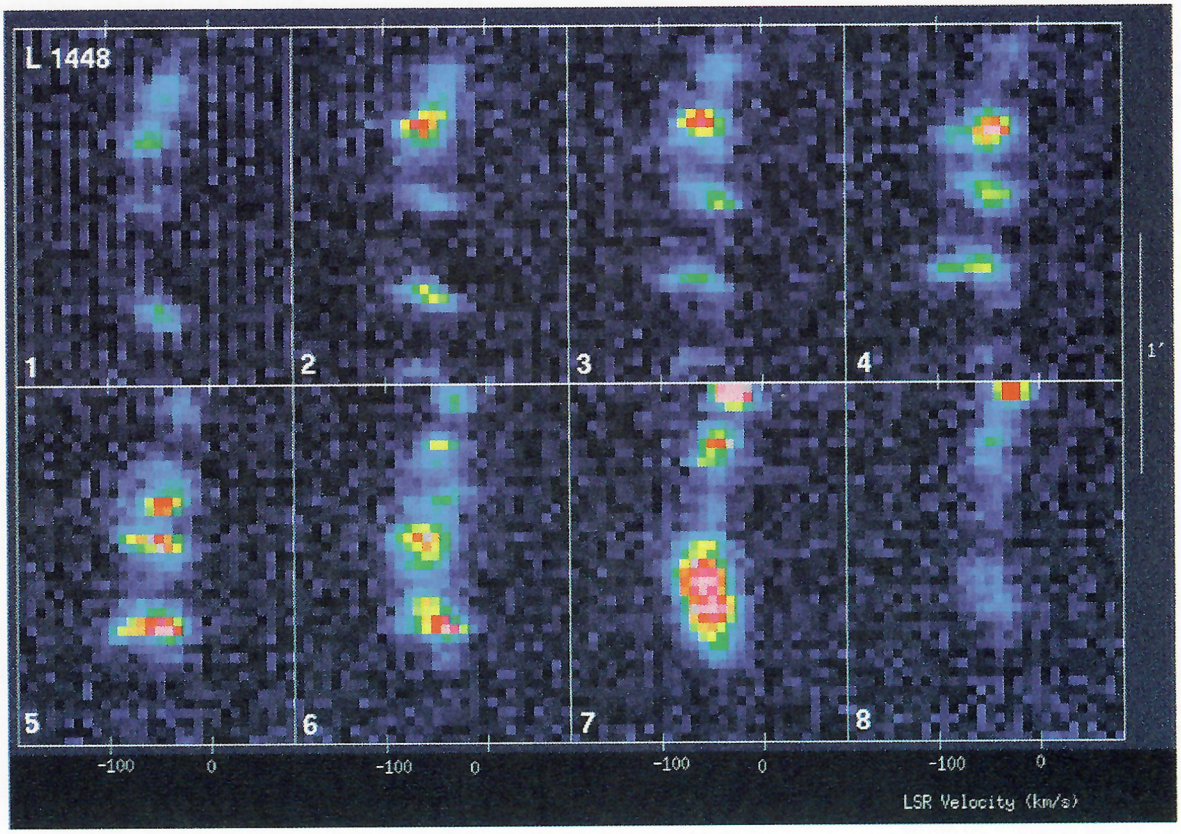

Fig. 3 – Near-IR, long slit spectra of the H_2 v = 1-0 S(1) line in L1448. The spectral resolution is 9.2 km s^{-1}; the spatial resolution 2.3 arcseconds. Eight slit positions were observed (p.a. = 118°), each shifted by 2 arcseconds in R.A. Position 1 to position 8 is from west to east; north-west is up.

ukirtinform

UKIRT observing schedules, news bulletins and other useful information can be found via the UKIRT WWW home page on **http://www.jach.hawaii.edu/UKIRT/home.html**.

New Fast Data-taking (Snapshot) Mode for IRCAM3

An important new mode of data-taking for the UKIRT common-user infrared camera IRCAM3 was commissioned on December 15, 1994. This mode, known as JOSE/snapshot, allows rapid permanent storage of individual frames at rates up to the array-limited speed and is intended for use in occultation and speckle observations and for the IR part of the JOSE atmospheric monitoring programme. This article provides an overview of the system and tabulates the limiting performance. Scientific results will be presented in future issues of *Spectrum*.

The JOSE/snapshot mode is now available as part of the IRCAM3 system for general use, in shared-risks mode for Semester 95A during further development of the user interface.

System overview

Data taken in the JOSE/snapshot mode may be temporarily stored in one of two locations, depending on the total volume of data, but in both cases is ultimately fed over a fibre-optic transputer link from IRCAM3's ALICE array control system to a SUN SPARC 5 containing a large amount of internal memory (256 Mbyte of RAM). At the end of the observation sequence, the data are transferred to a hard disk and then to a permanent storage device (presently a DAT drive).

If the data volume is small, less than 30 Mbyte, the data are first stored in local ALICE memory. This is the fastest mode of operation and ensures that all of the acquired data are stored. For larger data volumes, up to 218 Mbyte, the data proceed directly across the fibre link into SUN memory. Depending on the exposure time selected and what other processing tasks are ongoing in ALICE and the SUN, some frames of data may be lost (actually, discarded) in the latter mode. However, each frame of data is tagged so a record of which particular frames are lost is kept. The "hit rate" (fraction of total frames successfully stored) is displayed on the ALICE movie screen and depends sensitively on the exposure time (see below). Also displayed on the movie screen are individual frames (optionally background subtracted) sampled from the data stream (not every frame is displayed) and updated at about 1Hz.

JOSE/snapshot performance

(a) Data volume > 30 Mbyte

Table 1 shows the maximum number of frames that can be taken in a single JOSE/snapshot observation (limited to 218 Mbyte by available RAM) as a function of the array readout area. The minimum exposure times are also given for the standard and fast modes of IRCAM3 operation (note that these exposure times are longer than the array-limited speed because of overheads associated with data transfer and storage). The final column gives the maximum length of a single observation for data acquired at the fastest rate. Of course, longer exposures may be taken and the maximum length of the observation increases proportionately.

At the end of the observation the data stored in SUN memory must be written to disk before another sequence of JOSE/snapshot data can be taken. This data storage process incurs an overhead of 0.25s/Mbyte.

(Sub-) array size	Min exposure time (ms) (standard/fast modes)	Image size (2byte/pixel)	Max no of frames in single obs	Max length of observation at fastest rate (s)
256 × 256	120 / 102	128 kbyte	1750	210 / 179
128 × 128	36 / 24	32 kbyte	7000	252 / 168
64 × 64	12.5 / 10	8 kbyte	28000	350 / 280
256 × 48	23 / 20	24 kbyte	9333	214 / 187

(Sub-) array size	Hit rate (fraction of frames stored / frames taken) for specified exposure times (in ms)				
256 × 256	49% (102ms)	57% (120ms)	68% (150ms)	79% (180ms)	100% (240ms)
128 × 128	47% (24ms)	65% (36ms)	90% (50ms		
64 × 64	73% (10ms)	89% (13ms)	99% (15ms)		
256 × 48	48% (20ms)	56% (23ms)			

Table 1 (Top) – Data volume > 30 Mbyte.
Table 2 (Bottom) – Fraction of frames successfully stored.

(Sub-) array size	Min exposure time (ms) (standard/fast modes)	Max no of frames in single obs	Max. length of observation at fastest rate (s)
256 × 256	120 / 72	239	28 / 17
128 × 128	36 / 21	959	34 / 20
64 × 64	12.5 / 6.5	3839	48 / 25
256 × 48	23 / 14	1279	29 / 18

Table 3 – Data volume ≤ 30 Mbyte

In this mode, the fraction of frames successfully stored (*ie* not discarded because of overriding processing requirements) is shown in table 2.

(b) Data volume ≤ 30 Mbyte

For small datasets, this mode is the most efficient as all frames are stored and the system can be operated at the array-limited speed. Table 3 displays the minimum exposure time and maximum number of frames as a function of the array readout area.

At the end of the observation the data stored in ALICE memory must be written across the transputer link to the SUN and onto disk before another sequence of JOSE/snapshot data can be taken. This data storage process incurs an overhead of 2s/Mbyte.

Thanks to Magnus Paterson, Archie Smillie and the JAC computing staff for their efforts in providing a working system on such a short timescale.

Phil Puxley, ROE, and Colin Aspin, JAC

UKIRTSERV News

The UKIRT service observing programme presents an opportunity for astronomers to have a short observational project (less than 2 hours including overheads) carried out by UKIRT staff astronomers. Service nights are scheduled on average every month; the schedule for Semester 95A is given below. Applications are received about a month in advance of the scheduled service night, so data may be obtained on very short timescales. Proposals received by UKIRTSERV are graded, and those which are successful are added to our target list where they remain until the project is completed or until the data is no longer required by the applicants. If you require any further information, or wish to be added to the mailing list, please contact **UKIRTSERV@roe.ac.uk**. The successful operation of the service programme relies on the enthusiastic participation of the referees and service observers, for which much thanks.

During 1994, the UKIRT service programme remained as popular as ever, with 110 proposals being submitted compared with a total of 99 received in 1993. Just less than half these proposals are 'self-contained' in the sense that the service observations alone will provide the answer to a specific question. Around one quarter of the observations requested are needed to supplement existing data sets before a firm conclusion can be drawn from the observations previously made during PATT time or at different wavelengths. A few monitoring proposals were received, for which observations are on-going. The remainder of the proposals are more speculative, intended as feasibility studies leading up to a full proposal to PATT, designed to test an instrument, observing technique or theory.

Suzanne Ramsay Howat, ROE

Current Scheduled UKIRT Service Runs

The UKIRT Service runs for Semester 95A are provisionally scheduled as follows. Many nights are shared with AIC/engineering and so dates, deadlines and instruments may change in subsequent reminders. Accepted observations remain in the queue, so please apply as early as possible to maximise scheduling flexibility.

Date	Instruments	Deadline (noon UT)
8 – 9 April	IRCAM; 1.5 nights	17 March
14 May	CGS4; 1 night	21 April
16 May	CGS4; 0.5 night	
18 May	CGS4; 0.5 night	
8 – 9 June	IRCAM or CGS4; 2 × 0.5 nights	19 May
15 June	CGS3; 0.5 nights	
18 – 19 June	CGS3; 2 × 0.5 nights	
5 – 7 July	IRCAM; 3 × 0.5 nights	16 June
23 July	CGS4; 0.5 nights	30 June

JKT Jupiter Images

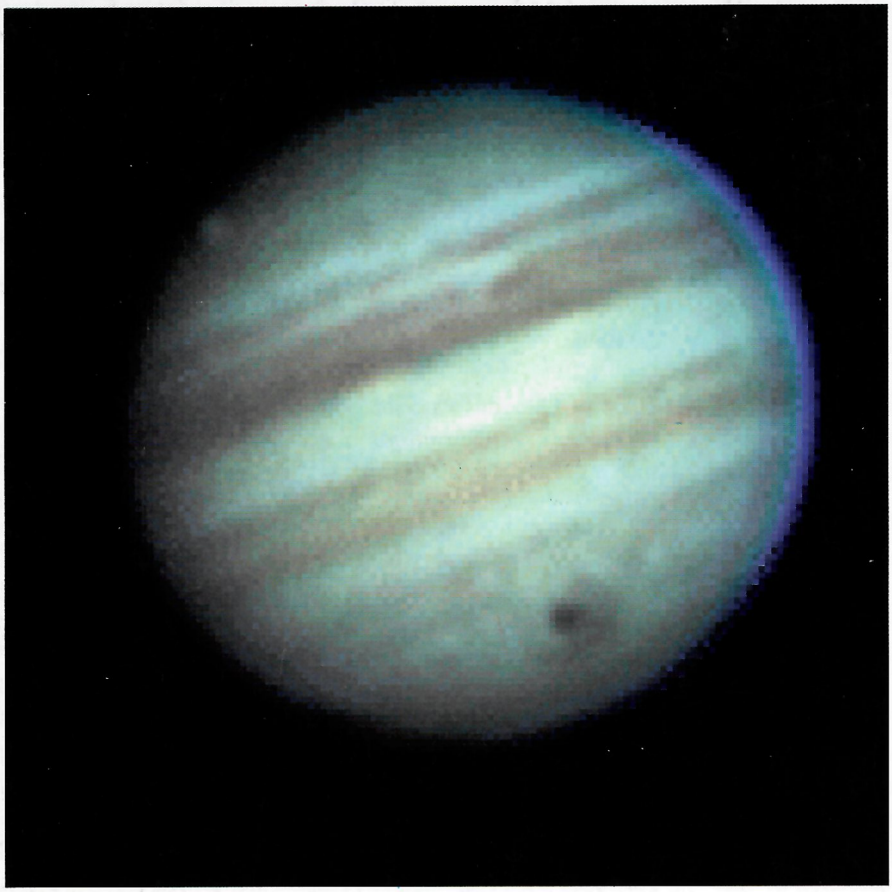

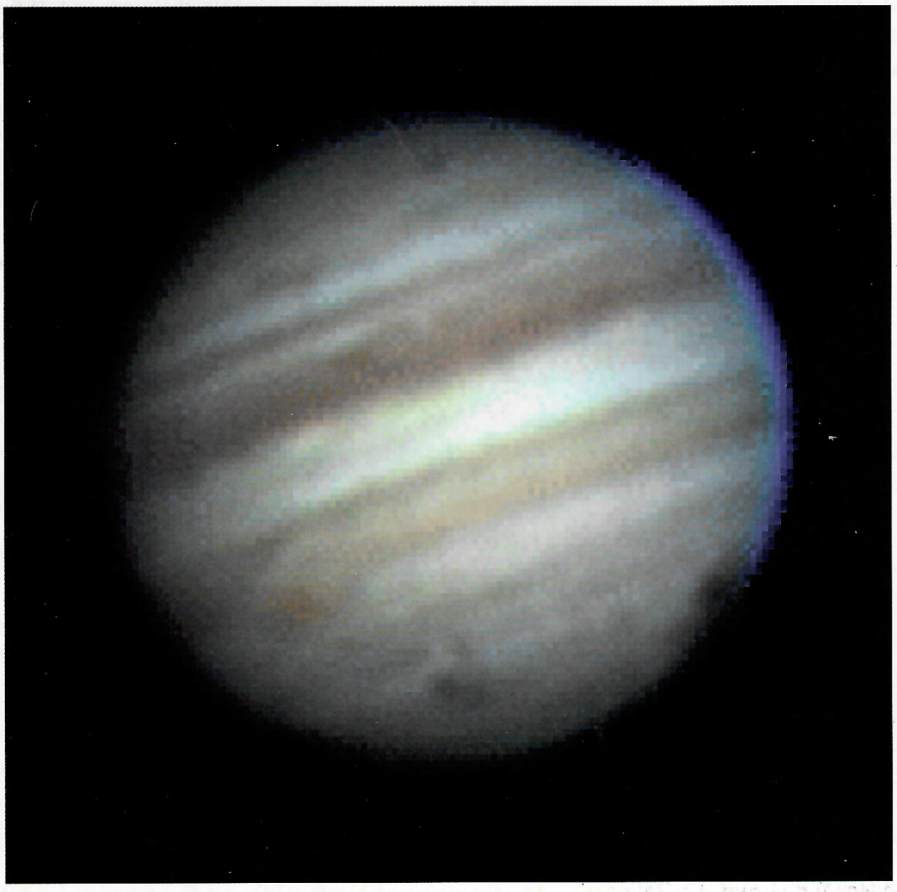

True colour images of Jupiter were obtained with the JKT on La Palma on the evening of 18 July 1994. Three narrow band images were calibrated and aligned using KAPPA routines on the Northern Ireland Starlink node, then added together within IDL to create this image. Many of the usual atmospheric features are visible, together with Jupiter's moon Ganymede just beginning to cross the upper left of the disk.

The large dark marking in the Southern hemisphere is from the impact of fragment G of comet Shoemaker-Levy 9, which had hit the planet exactly 14 hours previously. The impact site itself is the unresolved dark central core. Surrounding this is an arc of material approximately 18 000 km across, which is probably the remains of the impact plume observed by HST having fallen back onto the stratosphere of the planet.

The second image was obtained 80 minutes after the first. The planets rapid rotation has moved the G impact site onto the edge of the visible disk, while the impact site from fragment H is now well in view. Although similar in appearance to G, this feature is only just over two hours old. The size of both sites can be compared to the great red spot, which has now appeared on the morning limb.

Alan Fitzsimmons,
Queen's University, Belfast